

 Open access • Journal Article • DOI:10.1021/ACS.JMEDCHEM.7B01444

Controlling Plasma Stability of Hydroxamic Acids: A MedChem Toolbox

— [Source link](#) 

[Paul Hermant](#), [Damien Bosc](#), [Catherine Piveteau](#), [Ronan Gealageas](#) ...+14 more authors

Institutions: [Pasteur Institute](#), [University of Rouen](#), [university of lille](#)

Published on: 24 Oct 2017 - [Journal of Medicinal Chemistry](#) (American Chemical Society)

Related papers:

- [Histone deacetylase 6 structure and molecular basis of catalysis and inhibition.](#)
- [Quantitative Structure–Activity Relationship Studies on Hydroxamic Acids Acting as Histone Deacetylase Inhibitors](#)
- [Histone deacetylases and their inhibitors in cancer, neurological diseases and immune disorders](#)
- [Hydroxamates: Relationships between Structure and Plasma Stability](#)
- [Predicting the activity of hydroxamic acid analogues](#)

Share this paper:    

View more about this paper here: <https://typeset.io/papers/controlling-plasma-stability-of-hydroxamic-acids-a-medchem-50sqzaac4q>



HAL
open science

Controlling Plasma Stability of Hydroxamic Acids: A MedChem Toolbox

Paul Hermant, Damien Bosc, Catherine Piveteau, Ronan Gealageas, Baovy Lam, Cyril Ronco, Matthieu Roignant, Hasina Tolojanahary, Ludovic Jean, Pierre-Yves Renard, et al.

► **To cite this version:**

Paul Hermant, Damien Bosc, Catherine Piveteau, Ronan Gealageas, Baovy Lam, et al.. Controlling Plasma Stability of Hydroxamic Acids: A MedChem Toolbox. *Journal of Medicinal Chemistry*, American Chemical Society, 2017, 60 (21), pp.9067-9089. 10.1021/acs.jmedchem.7b01444 . hal-03054238

HAL Id: hal-03054238

<https://hal.archives-ouvertes.fr/hal-03054238>

Submitted on 11 Dec 2020

HAL is a multi-disciplinary open access archive for the deposit and dissemination of scientific research documents, whether they are published or not. The documents may come from teaching and research institutions in France or abroad, or from public or private research centers.

L'archive ouverte pluridisciplinaire **HAL**, est destinée au dépôt et à la diffusion de documents scientifiques de niveau recherche, publiés ou non, émanant des établissements d'enseignement et de recherche français ou étrangers, des laboratoires publics ou privés.

Controlling Plasma Stability of Hydroxamic Acids: A MedChem Toolbox.

Paul Hermant,^{#1} Damien Bosc,^{#1} Catherine Piveteau,^{#1} Ronan Gealageas,¹ BaoVy Lam,¹ Cyril Ronco,¹ Matthieu Roignant,¹ Hasina Tolojanahary,¹ Ludovic Jean,² Pierre-Yves Renard,² Mohamed Lemdani,³ Marilyne Bourotte,¹ Adrien Herledan,¹ Corentin Bedart,¹ Alexandre Biela,¹ Florence Leroux,¹ Benoit Deprez,¹ Rebecca Deprez-Poulain ^{*,1,4}

1. Univ. Lille, Inserm, Institut Pasteur de Lille, U1177 - Drugs and Molecules for Living Systems, F-59000 Lille, France; 2. Normandie Université, COBRA, UMR 6014 & FR 3038, Université de Rouen, INSA Rouen, CNRS, F-76821 Mont-Saint-Aignan Cedex, France.; 3 Univ. Lille. EA 2694 - Santé publique : épidémiologie et qualité des soins. F-59000 Lille. France. Institut 4. Institut Universitaire de France, F- 75231, Paris, France.

Abstract

Hydroxamic acids are outstanding zinc chelating groups that can be used to design potent and selective metalloenzyme inhibitors in various therapeutic areas. Some hydroxamic acids display a high plasma clearance resulting in poor *in vivo* activity, though they may be very potent compounds *in vitro*. We designed a 57-member library of hydroxamic acids to explore the structure-plasma stability relationships in these series and identify both which enzyme(s) and which pharmacophores are critical for plasma stability. Arylesterases and carboxylesterases were identified as the main metabolic enzymes for hydroxamic acids. Finally, we suggest structural features to be introduced or removed to improve stability. This work provides thus the first medicinal chemistry toolbox (experimental procedures and structural guidance) to assess and control the plasma stability of hydroxamic acids and realize their full potential as *in vivo* pharmacological probes and therapeutic agents. This study is particularly relevant to preclinical development as it allows to obtain compounds equally stable in human and rodent models.

Introduction

The hydroxamic acid function is a strong zinc chelating group. It can be used to design potent and selective metalloenzymes inhibitors that can serve both as biological probes¹ and leads. Hydroxamic acids can also be used as bioisosters of carboxylic acid thanks to their weak acid properties.² In the field of infectious diseases, several hydroxamic acid series have been reported as antibacterials : inhibitors of peptide deformylase (PDF)³, inhibitors of the neurotoxin A metalloprotease of bacterium *Clostridium botulinum* (BoNTA)⁴, or inhibitors of UDP-3-*O*-(*R*-3-hydroxymyristoyl)-*N*-acetylglucosamine deacetylase (LpxC) of gram-negative bacteria.⁵ Antivirals targeting HCV replication via a yet unknown mechanism,⁶ HIV integrase inhibitors,⁷ or inhibitors of metalloproteases of the *Plasmodium falciparum* parasite,⁸ have also been disclosed. Recently, inhibitors of the essential nematode-specific metalloprotease DPY-31 were discovered via combined *in silico* and experimental methods.⁹ Several groups have explored the use of hydroxamic acids in other therapeutic areas inhibitors of glutamate carboxypeptidase II (GCPII) in neuropathic pain;¹⁰ inhibitors of Insulin-Degrading Enzyme in type-2 diabetes¹¹, inhibitors of Matrix metalloprotease (MMP) in fibrinolysis control¹². In osteoarthritis, matrix-metalloproteinase¹³ or aggrecanase inhibitors¹⁴ have been proposed, while inhibitors of Tumor Necrosis Factor Converting Enzyme (TACE, ADAM17) were designed for autoimmune diseases such as psoriasis or Crohn's disease.¹⁵⁻¹⁶ In the area of cancer, several hydroxamic acids have been designed to inhibit various proteases such as the sheddase of HER-2.¹⁷ Importantly, with the growing interest in epigenetics, many teams explored the possibility to inhibit other zinc hydrolases, like histone deacetylases (HDACs). Several hydroxamic acid inhibitors of these targets have already been approved: vorinostat, and belinostat for T-cell lymphoma and recently panobinostat for multiple myeloma (Figure 1). Many other hydroxamic acids are currently following on these first clinical successes, not only in cancer, but also in several other therapeutic areas.¹⁸⁻¹⁹

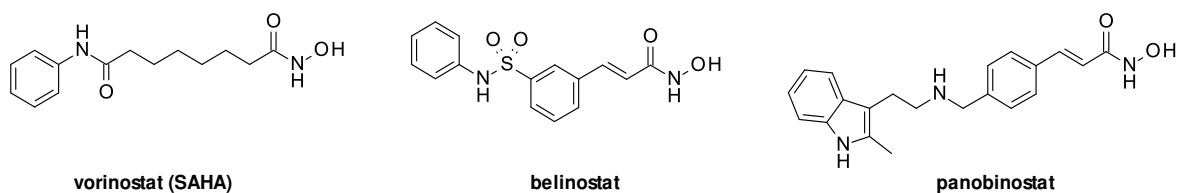


Figure 1: Marketed hydroxamic acid drugs.

The hydroxamic acid function undergoes phase I and phase II metabolism: it is mainly hydrolysed to the corresponding carboxylic acid,²⁰ but also it can be reduced to the corresponding amide²¹, O-glucuronylated or O-sulfated²². The carboxylic acid is usually much less active on the target and possesses different physical-chemical and permeability properties, than its hydroxamic acid analogue.²³ Depending on the fragility of the hydroxamic acid function, and the substituents in α - or β -position,²⁴ metabolism is driven towards the production of carboxylic acid, or the production of O-glucuronides. For example, the main metabolite of belinostat is the glucuronide form.²⁵

We and other groups have tried to improve the pharmacokinetics properties of hydroxamic acids thanks to chemical modulation.^{8,26} We have published a preliminary study of *in vitro* structure-plasma stability relationships (SPSR) of such compounds.²⁴ Here, we show that susceptibility to the esterase activity in plasma is a critical driver of the stability of hydroxamic acids.

Although often overlooked, esterases are worth considering in medicinal chemistry as they are involved in the metabolism of 10% of drugs.²⁷ Also, in specific situations, esterase activity can be used to release a parent drug from the ester prodrug (e.g. angiotensin-converting enzyme inhibitors, oseltamivir, tenofovir disoproxil)²⁸ or to inactivate rapidly a compound like in the soft-drug strategy²⁹ (ROCK inhibitors³⁰). Esterases can be sorted in two main types. Type A (arylesterases) includes paraoxonase-1 (PON-1) and other aryl esterase activities. Type B (serine esterases) includes acetyl- and butyl-cholinesterases (AChE and BuChE) as well as carboxylesterases (CES1 and 2) (Table 1). Along with these main enzymes, other esterases like arylacetamide deacetylase and acylpeptide hydrolase have been described.²⁷ Last but not least,

albumin, which is the most abundant protein in plasma, possesses a pseudo-esterase activity resulting in acylation of several of its nucleophilic residues such as Tyr411.³¹

Table 1: Esterases classification.^a

	Type A esterases		Type B esterases			Others
Acro Name	Paraoxonase	Other aryl esterase activities	Cholinesterases		Carboxylesterases	Albumine
Acro nym	PON1	ArE	AChE	BuChE	CES	SA
EC#	3.1.8.1	3.1.1.2	3.1.1.7	3.1.1.8	3.1.1.1	6.1.1.16
Catalytic mechanism	Catalytic dyad His/His Ca ²⁺ activated	undefined	Serine catalyzed Catalytic triad Ser, Glu, His			Irreversible acetylation of Tyr411 and other residues
Substrates & Inhibitors						
Substrates	RCOAr R ₁ O (R ₂ O)-PO-OAr	RCOOPh	CH ₃ COOR	BuCOOR, AlkCOOR	numerous prodrugs R ₁ COOR ₂	CH ₃ COOR
Selective Inhibitors	EDTA	DTNB	PMSF; tacrine; huprine	PMSF; tacrine; profenamine	PMSF; BNPP	undefined

^a EDTA: Ethylenediaminetetraacetic acid; DTNB: 5,5-dithio-bis-(2-nitrobenzoic acid); PMSF: Phenylmethylsulfonyl fluoride; BNPP: bis-para-nitrophenylphosphate.

These enzymes display different substrate specificities (Table 1). Using a histidine dyad,³² PON-1 hydrolyzes both arylesters and phosphotriesters and is inhibited by chelating agents such as EDTA. On the opposite, other plasma arylesterase activity do not have the ability to cleave the phosphotriesters³³ and are inhibited by 5,5'-dithiobis(2-nitrobenzoic acid) (DTNB).³⁴ BuChE displays a larger hydrophobic pocket that accounts for its less stringent substrate specificity over AChE. Both AChE and BuChE are inhibited by phenylmethylsulfonyl fluoride (PMSF), an irreversible inhibitor of serine proteases and tacrine, a prototypal cholinesterase inhibitor, or by specific non-covalent inhibitors (huprines³⁵ and profenamine respectively). CES1 and 2 are both inhibited by PMSF and bis-(4-nitrophenyl)-phosphate (BNPP) but CES1 recognizes substrates with either small or large acyl groups.³⁶

Importantly, tissue distribution of these enzymes differs among species,³⁷ in particular in plasma.³⁸⁻³⁹ While CES are the major esterases in rodent plasma, they are absent in human plasma.⁴⁰ On the contrary, AChE and BuChE are present at lower concentrations in rodent plasma. The major esterase in human plasma is BuChE while AChE is only present in trace amounts.⁴¹ Along with the plasma isoform of AChE, the E isoform of AChE (also called H for hydrophobic) is found in erythrocytes.⁴² Interestingly, PON-1 which is associated to HDL, displays a high polymorphism that impacts its expression and activity.^{32,43} Moreover, along with a presence in the serum, some esterases can be found in both liver and intestine. Importantly, CES1 is largely expressed in liver microsomes while CES2 is expressed in intestine microsomes,⁴⁰ where they participate actively in drug metabolism.²⁸ For these enzymes also, species differences in distribution have been reported.^{39,40}

Compounds that are unstable in plasma tend to display a high clearance, resulting in poor oral bioavailability and thus poor or undetectable activity, though they may be very potent compounds *in vitro*. The utility of such compounds as tools to probe *in vivo* pharmacokinetic/pharmacodynamic relationships in animal disease models in early drug-discovery is thus compromised.⁴⁴

The goal of this study is to establish Structure Plasma Stability Relationships (SPSR), identify enzymes at play in hydrolysis, and provide structural guidance to chemists in the design of hydroxamic acids that show sufficient stability in rodents. Obtaining hydroxamates that are equally stable in rodent and human is key to engage the target in preclinical disease models at the lowest dose, generate animal proof-of-principle and make a first assessment of the safety window. This is of particular importance as rodent plasma is much more aggressive to hydroxamic acids than human plasma, a cause of poor systemic exposure in preclinical models. A common practice in drug discovery is to optimize compounds potency on both a human target and its rodent ortholog, as well as stability on human and rodent liver microsomes to allow for

a proof of concept in animal models. Optimization of rodent plasma stability is of similar importance for the particular case of hydroxamic acids, even if the lead compound is already stable in human plasma.

In order to provide medicinal chemists with tractable information for improving stability of hydroxamic acids, we report here a set of protocols and results (the toolbox) that comprises tools to assess plasma stability of hydroxamic acids, structure-plasma stability relationships and dashboards for the identification of involved esterases.

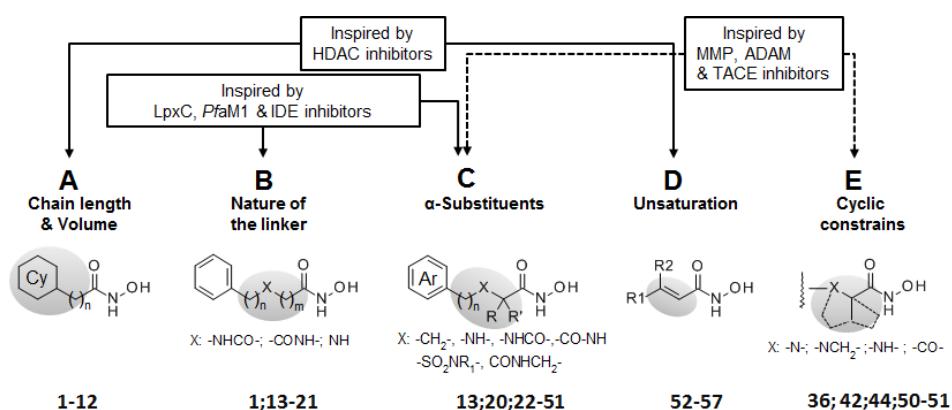


Figure 2: Hydroxamic acid library design.^a

^a $n = 0-6$; $m = 1-3$; In gray highlight: diversity within each hydroxamic acid library subset; Cy = Bz or cHx or adamantyl; Ar = Bz, p-fluorobenzyl, 4-pyridinyl, biphenyl, heteroaryl.

Results

Library Design.

To maximize the relevance of our study for medicinal chemists, we selected substructures found in a wide range of biologically active hydroxamic acids. The resulting 57-member library inspired from inhibitors of several classes of Zn metallohydrolases, allows in turn to explore different esterase pockets. We study the impact of chain length and volume (**1-12**, Figure 2A), nature of the linker (**1,13-21**, Figure 2B); α -substituents (**13,20,22-51**, Figure 2C); unsaturation (**52-57**, Figure 2D) and cyclic constraints (**36,42,44,50-51**, Figure 2E), and compare compounds.

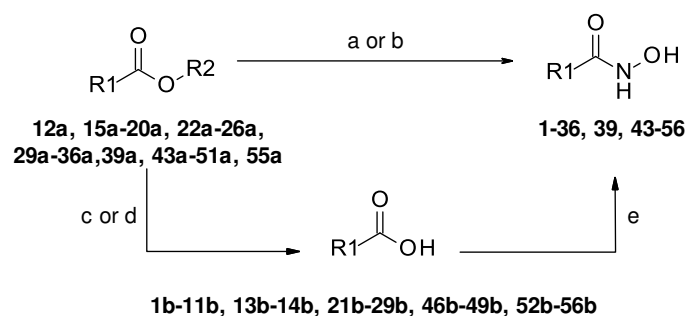
Among the compounds selected, linear alkyl hydroxamic acid series (Figure 2A) with various chain length and terminal cycles or linkers (Figure 2B) have been partially inspired by HDAC inhibitors and BoNTA inhibitors.⁴ Diversely α -substituted hydroxamic acids (Figure 2C) were inspired by *PfAM1* malonic inhibitors,⁸ LpxC inhibitors⁴⁵ and *hIDE* inhibitors¹¹. Other compounds were selected by homology to sulfonamides or sulfone-derived inhibitors of matrix-metalloproteases (MMP).⁴⁶ Hydroxamic acids inspired by inhibitors of aggrecanases (AGG)⁴⁷ or TACE^{48,16} were also designed and synthesized. Series of compounds with an unsaturation in α -position of the hydroxamic acid function (Figure 2D) have been inspired by cinnamic HDAC inhibitors⁴⁹⁻⁵⁰, *PfAM1* inhibitors⁸, or BoNTA inhibitors⁴. Finally, a number of hydroxamic acids displaying cyclic constraints in α -position (Figure 2E) complete the library. They were inspired by MMP⁵¹⁻⁵², LpxC⁵³ and TACE⁵⁴ inhibitors.

Synthesis of the library.

The studied **1-57** compounds were obtained either as previously described²⁴ (**37-38**, **40-42**, **57**) or via diverse synthetic approaches (**1-36**, **39**, **43-56**) summarized in schemes 1-7. Hydroxamic acids, scheme 1, were obtained either from the corresponding carboxylic acid by coupling with *O*-tritylhydroxylamine,⁵⁵ or from the corresponding ester by aminolysis with either hydroxylamine hydrochloride and KOH⁵⁶ or hydroxylamine and catalytic KCN⁵⁷ (**12**, **15-17**, **19-20**, **30-37**, **39**, **43-45**, **50-51**). Non-commercial precursors (**22b-29b**, **46b-49b**, **52b**, **54b-56b**) were synthesized as described in schemes 2-7.

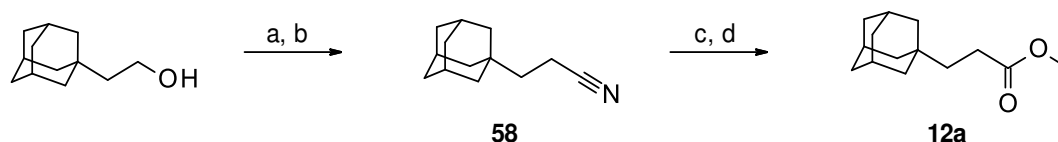
Commercial 2-(adamantan-1-yl)ethan-1-ol was tosylated and the resulting sulfonate was substituted using cyanide to afford **58**. Then, the nitrile was hydrolyzed under basic conditions giving the corresponding carboxylic acid, which was converted into the methyl ester **12a** (Scheme 2).

Scheme 1. From carboxylic acid or ester precursors to final hydroxamic acids.^a



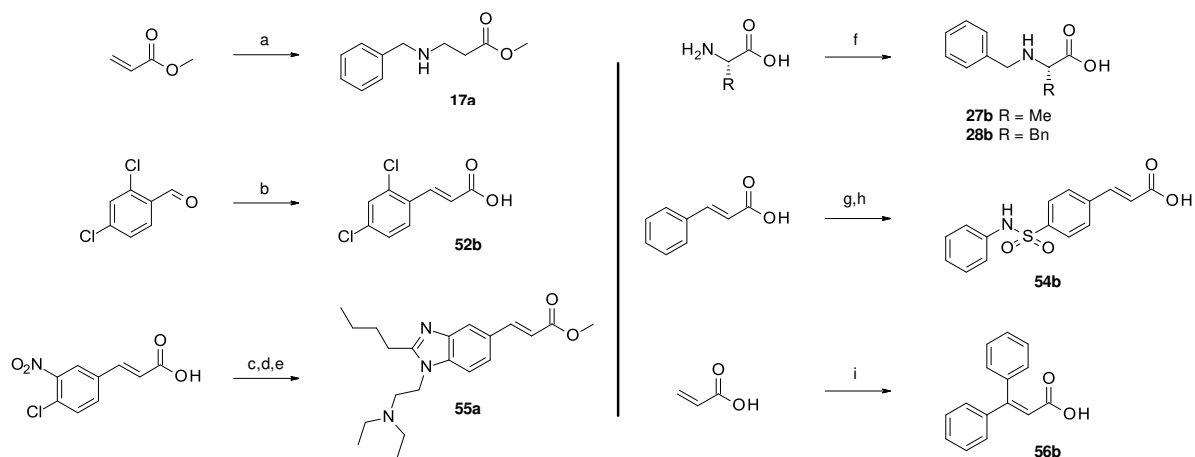
^a Reagents and conditions: (a) KCN, aq. NH₂OH 50 wt.%, MeOH, room temp., 2 h – 48 h, 4%-88% ; (b) NH₂OH.HCl, KOH, MeOH, room temp., 16 h, 36% yield for **18**; (c) (i) 2M NaOH, EtOH/THF, room temp., 16 h, (ii) 1N HCl, 52%-99%; (d) TFA, CH₂Cl₂, room temp., 2 h, quantitative yield; (e) (i) *O*-tritylhydroxylamine, EDCI, HOBT, *N*-methylmorpholine, DMF, room temp., 16 h; (ii) TFA, TIS, CH₂Cl₂, room temp., 15 min, 8%-99%.

Scheme 2. Synthesis of adamantane derivative **12a**.^a



^a Reagents and conditions: (a) 4-methylbenzenesulfonyl chloride, pyridine, room temp., 20 h, 75%; (b) KCN, DMF, 80 °C, 15 h, 84%; (c) KOH, EtOH, H₂O, 90 °C, 20 h, 97%; (d) SOCl₂, MeOH, 0 °C to room temp., 4 h, 21%.

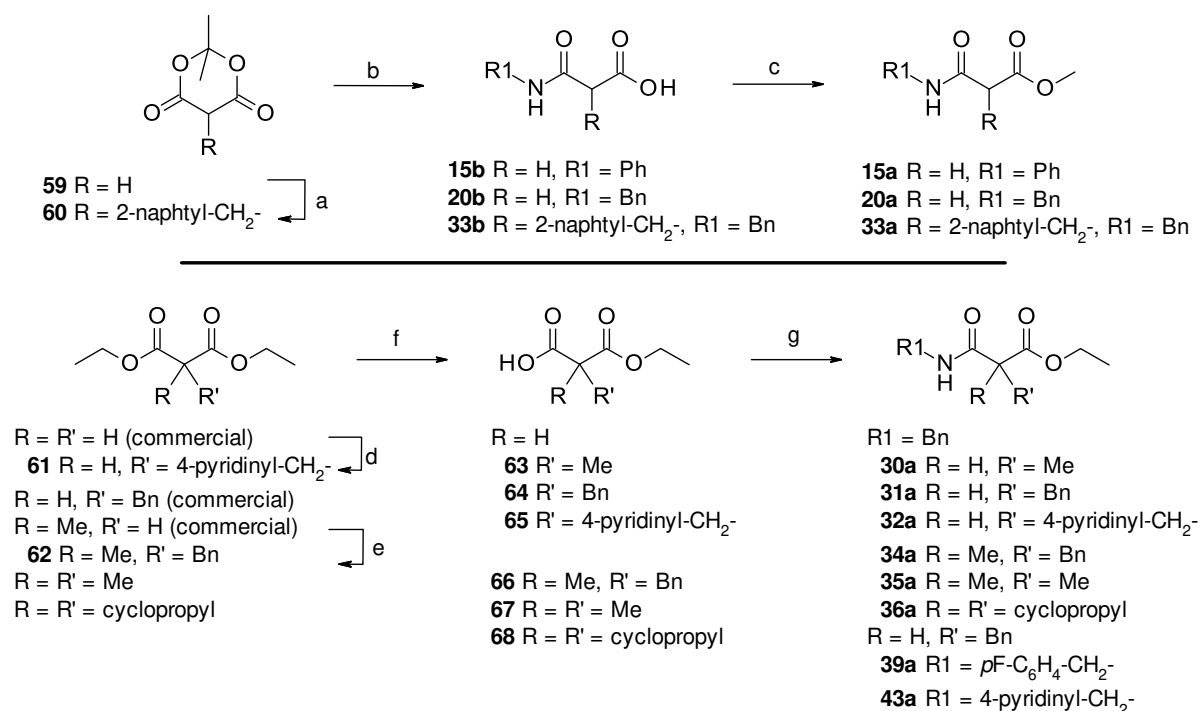
Scheme 3. Synthesis of the secondary amines **17a**, **27b-28b** and cinnamyl precursors **52b**, **54b**, **55a** and **56b**.^a



^a Reagents and conditions: (a) benzylamine, EtOH, room temp., 18 h, 84%; (b) malonic acid, pyridine, reflux, 1 h, quantitative yield; (c) MeOH, H₂SO₄, reflux, 16 h, 79%; (d) *N,N*-diethylethylenediamine, Et₃N, dioxane, 90 °C, 16 h, 65%; (e) valeraldehyde, SnCl₂·2H₂O, AcOH, MeOH, 40 °C, 16 h, 48%; (f) (i) LiOH·H₂O, MeOH, room temp., 20 min, (ii) benzaldehyde, room temp., 1 h, (iii) NaBH₄, room temp., 30 min, 76%-100%; (g) chlorosulfonic acid, 10-12 °C, 16 h, 30%; (h) aniline, pyridine, CH₂Cl₂, room temp., 16 h, 66%; (i) iodobenzene, silver acetate, palladium acetate, acetic acid, 110 °C, 6 h, 61%.

Hydroxamic acid analogs bearing a secondary amine (**17**, **27** and **28**) or a cinnamyl moiety (**52** and **55**) were synthesized as described in Scheme 3. The linear ester precursor **17a** was obtained via an aza-Michael reaction whereas a reductive amination from benzaldehyde and the corresponding amino-acid afforded acidic precursors **27b** and **28b**.⁵⁸ Benzenepropenoic acids **54b** and **55a**, analogues of HDAC inhibitors, were obtained according to the literature.⁴⁹⁻⁵⁰ Compound **52b**, the acid precursor of a botulinum neurotoxin A protease inhibitor⁵⁹ was synthesized by a Döbner-Knöevenagel condensation from malonic acid and 2,4-dichlorobenzaldehyde. At last, disubstituted alkene **56b** was synthesized by palladium-catalyzed Heck diarylation⁶⁰ (Scheme 3).

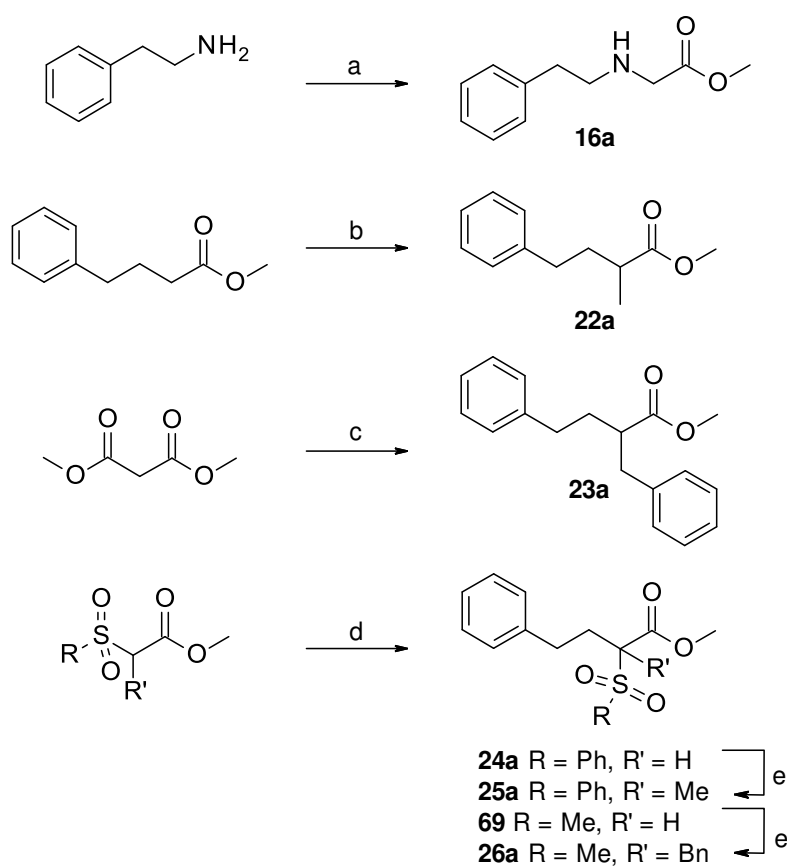
Scheme 4. Synthesis of malonic precursors.^a



^a Reagents and conditions: (a) (i) 2-naphthaldehyde, MeCN, room temp., 1.5 h, (ii) Hantzsch's ester, L-proline, MeOH, room temp., 16 h, 68%; (b) aniline, MeCN, 80 °C, 2 h, 48% **15b**, benzylamine, MeCN room temp., 3 h, 63% **20b**, benzylamine, MeCN, MW 80 °C, 1.75 h, 95% **33b**; (c) SOCl₂, MeOH, 0 °C to room temp., 0.5-5.25 h, 43%-89%; (d) (i) NaH, THF, 0 °C to room temp., 30 min, (ii) 4-(chloromethyl)pyridine hydrochloride, 40 °C, 5.5 h, 23%; (e) (i) Sodium, abs. EtOH, 0 °C to 50°C, 1 h, (ii) bromomethylbenzene, 50 °C, 19 h, 37%; (f) KOH, EtOH, room temp., 24 h, quantitative yield; (g) amine, HBTU, DIPEA, DMF, 0 °C to room temp., 4h-18h, 41%-75%.

Malonic precursors were synthesized to explore the impact of substitution in α -position of the hydroxamic acid function. A one-pot Knoevenagel-reduction catalyzed by L-proline gave precursor **60**.⁶¹ The dissymmetric opening of the Meldrum's acids **59** and **60** with primary amines, and subsequent methyl esterification, afforded **15a**, **20a**, and **33a**. Precursors **61** and **62** were obtained via alkylation of commercial malonic esters. Mono-saponification, followed by coupling with the corresponding amine resulted in compounds **30a-32a**, **34a-36a**, **39a**, **43a** (Scheme 4).

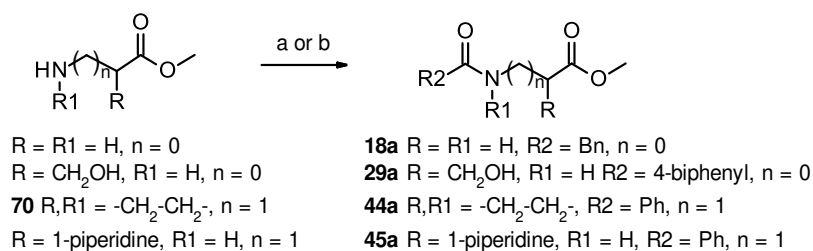
Scheme 5. Synthesis of phenylalkyl ester precursors **16a**, **22a-26a**.^a



^a Reagent and conditions: (a) methyl-2-bromoacetate, DIPEA, DMF, 0 °C to room temp., 4 h, 54%; (b) LDA, MeI, THF, -78 °C to room temp., 85%; (c) (i) (2-iodoethyl)benzene, NaH, DMF, 70 °C, 3.5 h, 79%, (ii) benzyl bromide, NaH, DMF, toluene, room temp., 60 h, 83%; (iii) KOH, 2-methoxyethanol/H₂O (10/1 v/v), 130 °C, 1.5 h, then 6N HCl, 83%. (d) (2-bromoethyl)benzene, NaH, DMF, 0 °C, 1 h then room temp., 16 h, 90%; (e) methyl iodide or bromomethylbenzene, NaH, DMF, 55 °C, overnight, 71%-78%.

Ester precursors **16a**, **22a-26a** were obtained as follows (Scheme 5). The 2-phenylethan-1-amine was alkylated by methyl-2-bromoacetate to give ester **16a**, while alkylation of methyl 4-phenylbutanoate with methyl iodide afforded compound **22a**. Alkylation of dimethyl malonate with (2-iodoethyl)benzene followed by hydrolysis and decarboxylation gave methyl ester **23a**. Treatment of ethyl (methylsulphonyl)acetate and ethyl (phenylsulphonyl)acetate with both sodium hydride and (2-bromoethyl)benzene afforded **69** and **24a** respectively. Phenylsulfonyl **24a** was alkylated with methyl iodide and sodium hydride to give **25a**. In a similar manner methylsulfonyl **69** was treated with benzyl bromide, giving **26a**.

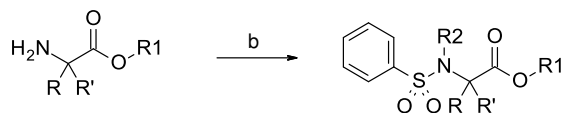
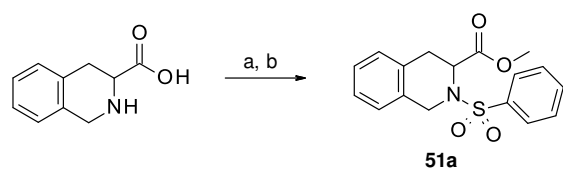
Scheme 6. Synthesis of amides **18a**, **29a**, **44a-45a**.^a



^a Reagent and conditions: (a) phenyl-acetic acid, HOBt, EDCI, DIEA, DMF, room temp., 12 h-48 h, 70%-84%; (b) benzoyl chloride, DIPEA, CH₂Cl₂, 0°C to room temp., 1 h-2 h, 41%-62%.

Ester precursors **18a**, **29a**, **44a** and **45a** were synthesized via acylation reactions (Scheme 6). Sulfonamides **46a-47a**⁴⁶ and **50a-51a**¹⁶ were synthesized by acylation with benzenesulfonyl chloride. At last, *D*-valine and *D*-phenylalanine underwent *N*-sulfonylation (**71**, **73**), followed by esterification (**72**, **74**) and *N*-alkylation to afford compounds **48a** and **49a** respectively (Scheme 7).

Scheme 7. Synthesis of sulfonlated precursors **46a-51a**.^a



50a R = R' = 4-oxane, R1 = Me, R2 = H
 R = *t*-Pr, R' = H
71 R1 = H, R2 = H
72 R1 = *t*-Bu, R2 = H
48a R1 = *t*-Bu, R2 = Bn
46a R1 = Et, R2 = H
 R = Bn, R' = H
73 R1 = H, R2 = H
74 R1 = *t*-Bu, R2 = H
49a R1 = *t*-Bu, R2 = Bn
47a R1 = Et, R2 = H

^a Reagents and conditions: (a) SOCl₂, MeOH, 0 °C to room temp., 10 days, 64%; (b) benzenesulfonyl chloride, base, solvent, 0 °C to room temp., 2 h-18 h, 24%-66%; (c) di-*tert*-butylacetal, toluene, DMF, 95 °C, 16 h, 65%-71%; (d) benzyl bromide, K₂CO₃, DMF, 2 days, room temp., 87%-96%.

Relations between chemical structure and plasma stability

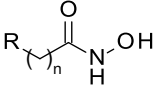
Compounds **1-57** were evaluated for their stability in both rat plasma and human plasma. Rat was chosen as its plasma displays high hydrolytic properties⁶² and it is a species often used for regulatory toxicology studies to determine therapeutic window. Half-lives in rat plasma are presented in four tables (2 to 5) highlighting the influence of chain length and composition, and nature of substituent in alpha to the hydroxamate function.

Linear compounds with saturated aliphatic linkers (1-7, Table 2): Several phenyl linear compounds were synthesized to explore the influence of the chain length on plasma stability of the hydroxamic acid function. Interestingly, when phenyl or benzyl substituents are directly linked to the hydroxamic acid function (n = 0 and 1), compounds are stable while the most unstable compounds were obtained with medium chain length (n=2, 3 and 4). Then compounds with aliphatic extended linear chain (n = 5, 6) have long half-lives (4-6 hours).

Cyclohexane (**8, 9-10**) and adamantane derivatives (**11, 12**) behave the same way as their phenyl analogues (**2-4**) (Table 2). Indeed, linker with n = 2 or 3 are hydrolysed rapidly in

plasma ($t_{1/2} < 0.5$ hours), while for $n = 1$, compounds are stable. Interestingly both lipophilicity and size impact the rate of hydrolysis. This is exemplified by the decreasing stabilities of adamantane **12** > cyclohexane **9** displaying cLogP of 2.2 and, 2.01 and molecular volume of 161 and 120 Å³ respectively.

Table 2: Influence of chain length, aromaticity and volume on plasma stability.

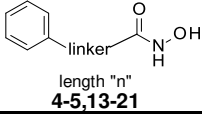


1-12

Cpd	R-	n	$t_{1/2}$ (h) ^a
1	Ph-	0	>6 ^b
2	Ph-	1	>6 ^b
3	Ph-	2	0.8 ^b
4	Ph-	3	2.0 ^b
5	Ph-	4	0.9
6	Ph-	5	4.5
7	Ph-	6	>6
8	cHx-	1	>6
9	cHx-	2	0.06
10	cHx-	3	0.05
11	Adamantyl-	1	>6
12	Adamantyl-	2	0.5

^a Half-life in rat plasma. ^bFrom reference 24.

Linear compounds with heteroatom-containing linkers(Table 3): Regardless of its size, the nature of the linear linker impacts plasmatic stabilities of hydroxamic acids. Indeed, half-lives vary from 0.6 to more than 6 hours for a 3-atom linker and from 0.3 to more than 6 hours for a 4-atom linker respectively. Interestingly, linear alkyl compounds **4** and **5** are not the most stable hydroxamic acids in the series. Introduction of a secondary amine is either beneficial for stability (**13** vs **4** or **17** vs **5**) or deleterious (**16** vs **5**). The presence of an amide function in β - or γ - position of the hydroxamic acid is critical for stability (**20** vs **21** and **18** vs **19**). Also, hydroxamic acids **14** and **18** derived of glycine are far less stable than their retro-amide analogs **15** and **20** respectively, which are the most stable compounds in the series (Table 3).

Table 3: Influence of the nature of the linear linker.

Cpd	Linker	“n”	t _{1/2} (h) ^a
4	-CH ₂ -CH ₂ -CH ₂ -	3	2.0 ^b
13	-CH ₂ -NH-CH ₂ -	3	3.6
14	-CO-NH-CH ₂ -	3	0.58
15	-NH-CO-CH ₂ -	3	>6
5	-CH ₂ -CH ₂ -CH ₂ -CH ₂ -	4	0.93
16	-CH ₂ -CH ₂ -NH-CH ₂ -	4	0.5
17	-CH ₂ -NH-CH ₂ -CH ₂ -	4	2.1
18	-CH ₂ -CO-NH-CH ₂ -	4	0.29
19	-CO-NH-CH ₂ -CH ₂ -	4	2.5
20	-CH ₂ -NH-CO-CH ₂ -	4	>6
21	-NH-CO-CH ₂ -CH ₂ -	4	0.43

^a Half-life in rat plasma. ^b From reference 24.

Impact of the substituent in α -position to the hydroxamate (Table 4): In the series of 4-phenylbutanehydroxamic acid **4**, introduction of a substituent in α -position results in a higher plasma stability (**22-26**). On the contrary, in 2-(benzylamino)ethanehydroxamic acid series (**13**, **27-29**) and malono-hydroxamic series (**20**, **30-43**), introduction of benzyl substituent or aryl-methyl groups is deleterious for stability (**28**, **31-34**, **39-40**, **43**), in comparison with smaller substituents like methyl (**27**, **30**, **38**). Interestingly, the size and nature of the aryl-methyl group in alpha positions impacts stability: pyridine > phenyl > naphthyl (**31-33**).

Surprisingly, groups at long distance from the hydroxamic acid can also impact stability. Indeed, pyridinyl compound **43** is much more stable (t_{1/2} = 3.3 h) than benzyl and *p*-fluorobenzyl analogues (**31**, **39**) (t_{1/2} = 0.8 h), although **43** contains a benzyl group in α -position, a substructure shown above to accelerate hydrolysis by plasma. Gem-dimethyl substitution or introduction of a cyclopropyl group allow obtention of stable compounds (**35-36**; **41-42**). Introduction of a methyl group in α -position moderately restores stability for benzyl-substituted compounds (**34** vs **31**; **40** vs **39**): t_{1/2} of 1.5 vs 0.8 hours. In the beta-alanine series (**44**, **19**, **45**), introduction of a cyclic constraints protects from hydrolysis (**44**, t_{1/2} > 6 h) while introduction of a positive charge results in poorly stable compound (**45** t_{1/2} = 0.4 h). In comparison with

these beta-alanine derivatives, serine-base compound **29** is stable. Finally, in the sulfonamide series the presence of an isopropyl group prevents hydrolysis (**46**, **48**) while a benzyl group promotes it (**47**). Interestingly, substitution of the nitrogen of the adjacent amide function by a benzyl group restores plasmatic stability (**49** vs **47**) but freezing α -position substituent with the amide substituent into a tetrahydroquinoline is deleterious for stability (**51**). As gem-substitution was tolerated in other series, it is also protective in sulfonamide series (**50**).

Table 4: Impact of substitution in α -position of the hydroxamic acid function.

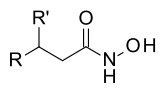
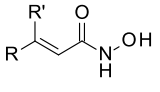
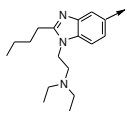
4,13,19,22-51

#	Ar-	n	X	-R'	-R	-R ₁	t _{1/2} (h) ^a
4	Ph-	1	CH ₂	-H	-H		2.0 ^b
22	Ph-	1	CH ₂	-H	-CH ₃		>6
23	Ph-	1	CH ₂	-H	-CH ₂ -Ph		>6
24	Ph-	1	CH ₂	-H	-SO ₂ -Ph		>6
25	Ph-	1	CH ₂	-SO ₂ -Ph	-CH ₃		>6
26	Ph-	1	CH ₂	-SO ₂ -CH ₃	-CH ₂ -Ph		>6
13	Ph-	1	NH	-H	-H		3.6
27	Ph-	1	NH	-H	-CH ₃		>6
28	Ph-	1	NH	-H	-CH ₂ -Ph		1.8
20	Ph-	1	NHCO	-H	-H		>6
30	Ph-	1	NHCO	-H	-CH ₃		>6
31	Ph-	1	NHCO	-H	-CH ₂ -Ph		0.8
32	Ph-	1	NHCO	-H	-CH ₂ -4-pyridinyl		4.5
33	Ph-	1	NHCO	-H	-CH ₂ -2-naphthyl		0.1
34	Ph-	1	NHCO	-CH ₃	-CH ₂ -Ph		1.5
35	Ph-	1	NHCO	-CH ₃	-CH ₃		>6
36	Ph-	1	NHCO	-cyclopropyl-	-cyclopropyl-		>6
37	<i>p</i> F-C ₆ H ₄ -	1	NHCO	-H	-H		>6
38	<i>p</i> F-C ₆ H ₄ -	1	NHCO	-H	-CH ₃		>6
39	<i>p</i> F-C ₆ H ₄ -	1	NHCO	-H	-CH ₂ -Ph		0.8 ^b
40	<i>p</i> F-C ₆ H ₄ -	1	NHCO	-CH ₃	-CH ₂ -Ph		1.5 ^b
41	<i>p</i> F-C ₆ H ₄ -	1	NHCO	-CH ₃	-CH ₃		>6 ^b
42	<i>p</i> F-C ₆ H ₄ -	1	NHCO	-cyclopropyl-	-cyclopropyl-		>6 ^b
43	4-pyridinyl-CH ₂ -	1	NHCO	-H	-CH ₂ -Ph		3.3
19	Ph-	0	CONHCH ₂	-H	-H	-H	2.5
44	Ph-	0	CONR ₁ CH ₂	-H	-CH ₂ -CH ₂ -		>6
45	Ph-	0	CONHCH ₂	-H	-piperidinyl	-H	0.4
29	4-biphenyl-	0	CONH	-H	-CH ₂ OH	-H	>6
46	Ph-	0	SO ₂ NR ₁	-H	-iPr	-H	>6 ^b
47	Ph-	0	SO ₂ NR ₁	-H	-CH ₂ -Ph	-H	0.1
48	Ph-	0	SO ₂ NR ₁	-H	-iPr	-CH ₂ -Ph	>6
49	Ph-	0	SO ₂ NR ₁	-H	-CH ₂ -Ph	-CH ₂ -Ph	>6
50	Ph-	0	SO ₂ NR ₁	-CH ₂ -CH ₂ -O-CH ₂ -CH ₂ -		-H	>6
51	Ph-	0	SO ₂ NR ₁	-H			0.7

^a Half-life in rat plasma. ^b From reference 24.

Introduction of a double bond in α -position of the hydroxamic acid impacts stability. For example, compound **57** is stable while its saturated analogue **3** is rapidly hydrolyzed ($t_{1/2} = 0.8$ h) (Table 5). Other unsaturated compounds inspired by bioactive structures are stable in rat plasma (Table 5).

Table 5: Influence of unsaturation.

			
Cpd	R	R'	$t_{1/2}$ (h) ^a
3	Ph-	H-	0.8
52	1,3-dichlorophenyl-	H-	>6
53	4-biphenyl-	H-	>6
54	p-(Ph-NHSO ₂)-C ₆ H ₄ -	H-	>6
55		H-	>6
56	Ph-	Ph	>6
57	Ph-	H-	>6 ^b

^a Half-life in rat plasma. ^b From reference 24.

Impact of physical-chemical properties on stability.

Table 6 presents the measured stability and physical chemical properties of the 57 hydroxamic acids. In an attempt to correlate these properties of compounds with plasma stability, we looked at the distribution of 6 continuous parameters for stable ($t_{1/2} > 6$ h) and unstable ($t_{1/2} < 6$ h) compounds: cLogP, cLogD_{7.4}, Polar Surface Area (PSA), aqueous solubility (cLogS), Molecular Weight and Volume. No difference of distribution between unstable and stable compounds were observed for cLogS, Volume or PSA. However, unstable hydroxamic acids tend to have a higher cLogP (36% of compounds with cLogP in [0;1.5[range and 52% with cLogP in [1.5 ; 3]) than stable compounds (50% of compounds with cLogP in [0;1.5[range and 28% with cLogP in [1.5;3]) (Supplementary Figure S8). The same difference in distribution is observed for cLogD (Supplementary Figure S8). This is well illustrated in the malonic-

derived hydroxamic acids **20-43** (Table 4) where compounds displaying short half-lives have a higher cLogP than those displaying a higher half-life. For example pyridine lowers cLogP in comparison with benzene, and also impacts positively stability (**32** and **43**).

We then performed an analysis including the (categorical) HBD and HBA parameters. Indeed, a Chi-square test showed a link between stability and HBD <3 ($p = 0.068$). This led us to perform a multivariate analysis using HBD along with the 6 other continuous variables. A stepwise logistic regression yielded a model with HBD, MW and Volume. It shows that HBD <3 favors stability ($OR = 4.80$), along with a higher molecular weight ($OR = 1.06$) and lower volume ($OR = 0.91$).

Table 6: Physical-chemical properties of compounds.

Cpd	t _{1/2} (h) ^a	cLogP ^b	cLogD ^b	PSA ^b	cLogS ^b	MW	Volume ^b	HBD ^c	HBA ^c
1	>6	0.84	0.83	49.3	-1.41	137.1	80.9	2	2
2	>6	0.88	0.87	49.3	-1.72	151.2	99.1	2	2
3	0.8	1.34	1.33	49.3	-2.13	165.2	108.7	2	2
4	2.0	1.79	1.79	49.3	-2.58	179.2	122.8	2	2
5	0.9	2.25	2.25	49.3	-3.07	193.2	131.7	2	2
6	4.5	2.70	2.70	49.3	-3.57	207.3	143.7	2	2
7	>6	3.16	3.16	49.3	-4.09	221.3	158.1	2	2
8	>6	1.55	1.55	49.3	-1.90	157.2	110.8	2	2
9	0.06	2.01	2.01	49.3	-2.41	171.2	121.4	2	2
10	0.05	2.46	2.46	49.3	-2.94	185.3	135.5	2	2
11	>6	1.77	1.77	49.3	-2.69	209.3	145.8	2	2
12	0.5	2.23	2.22	49.3	-3.27	223.3	159.5	2	2
13	3.6	0.23	-0.34	61.4	-1.89	180.2	119.7	3	3
14	0.58	-0.10	-0.24	78.4	-1.81	194.2	119.7	3	3
15	>6	0.15	0.15	78.4	-1.83	194.2	121.8	3	3
16	0.5	0.56	-0.01	61.4	-2.34	194.2	129.7	3	3
17	2.1	0.48	-1.41	61.4	-2.23	194.2	129.3	3	3
18	0.29	-0.06	-0.20	78.4	-2.10	208.2	131.7	3	3
19	2.5	0.15	0.15	78.4	-2.00	208.2	132.1	3	3
20	>6	0.15	0.15	78.4	-2.15	208.2	131.0	3	3
21	0.43	0.18	0.18	78.4	-1.99	208.2	132.1	3	3
22	>6	2.25	2.25	49.3	-2.95	193.2	133.8	2	2
23	>6	3.74	3.74	49.3	-5.00	269.3	181.4	2	2
24	>6	2.72	2.87	91.9	-4.44	319.4	199.6	2	4
25	>6	3.03	3.02	91.9	-4.61	333.4	212.3	2	4
26	>6	3.01	3.00	91.9	-4.91	347.4	225.4	2	4
27	>6	0.72	0.12	61.4	-2.31	194.2	130.0	3	3
28	1.8	2.27	2.26	61.4	-4.30	270.3	180.4	3	3
29	>6	1.02	0.99	98.7	-4.05	300.3	180.4	4	4
30	>6	0.62	0.63	78.4	-2.67	222.2	143.4	3	3
31	0.8	2.10	2.12	78.4	-4.50	298.3	192.8	3	3
32	4.5	0.95	0.95	91.3	-4.04	299.3	190.4	3	4
33	0.1	3.01	3.03	78.4	-6.20	348.4	226.0	3	3
34	1.5	2.52	2.52	78.4	-4.76	312.4	204.8	3	3
35	>6	1.03	1.03	78.4	-2.95	236.3	155.0	3	3

36	>6	0.66	0.66	78.4	-2.49	234.3	148.2	3	3
37	>6	0.36	0.35	78.4	-2.45	226.2	137.9	3	3
38	>6	0.82	0.83	78.4	-2.98	240.2	152.6	3	3
39	0.8 ^b	2.31	2.32	78.4	-4.77	316.3	198.9	3	3
40	1.5 ^b	2.73	2.73	78.4	-5.01	330.4	212.7	3	3
41	>6 ^b	1.24	1.24	78.4	-3.24	254.3	165.7	3	3
42	>6	0.87	0.87	78.4	-2.77	252.2	154.0	3	3
43	3.3	0.95	0.95	91.3	-4.03	299.3	190.7	3	4
44	>6	0.41	0.41	69.6	-1.75	234.3	149.2	2	3
45	0.4	1.10	0.64	81.7	-2.67	291.4	193.5	3	4
46	>6	0.93	0.93	103.9	-2.87	272.3	167.7	3	4
47	0.1	1.65	1.64	103.9	-4.06	320.4	193.8	3	4
48	>6	2.72	2.71	95.1	-4.61	362.4	236.0	2	4
49	>6	3.44	3.43	95.1	-5.77	410.5	257.6	2	4
50	>6	-0.48	-0.48	113.1	-2.00	300.3	182.8	3	5
51	0.7	1.61	1.61	95.1	-3.60	332.4	200.7	2	4
52	>6	2.64	2.64	49.3	-3.96	232.1	136.5	2	2
53	>6	2.83	2.83	49.3	-4.75	239.3	150.9	2	2
54	>6	1.80	1.80	103.9	-4.36	318.4	192.1	3	4
55	>6	3.71	2.28	70.4	-5.80	358.5	256.6	2	4
56	>6	2.79	2.79	49.3	-4.30	239.3	148.9	2	2
57	>6	1.31	1.31	49.3	-2.41	163.2	99.1	2	2

^a Half-life in rat plasma. ^b cLogP, cLogD, PSA in Å², S in mol/L, Volume in Å³ calculated by PipelinePilot. ^c Hydrogen-bond donors; Hydrogen-bond acceptors.

Implication of esterases

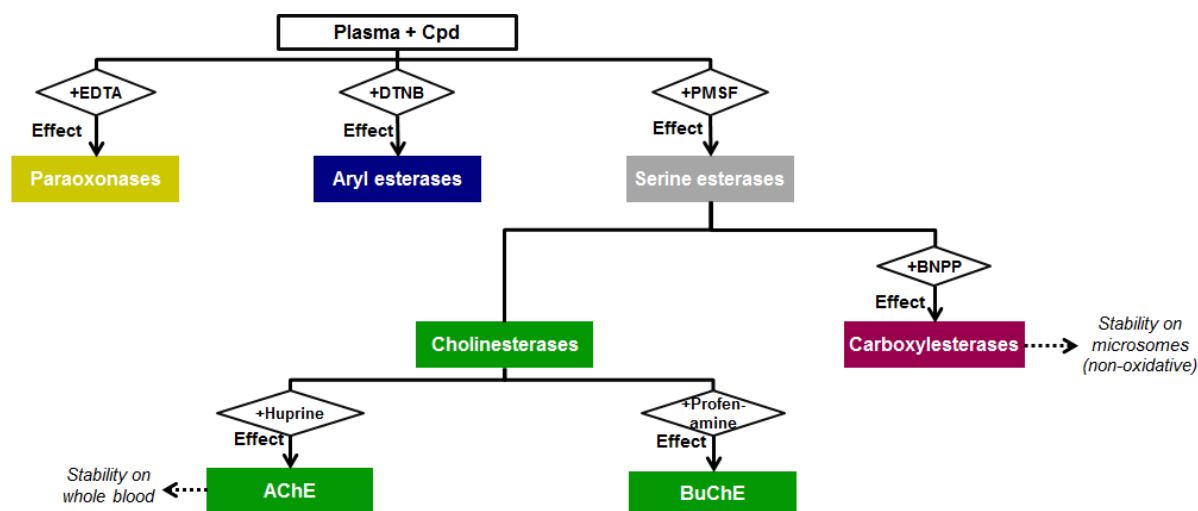


Figure 3: Inhibitor-based esterase profiling scheme.

To find which esterase(s) was (were) responsible for the hydrolysis of the unstable compounds, and attempt to rationalize SPSR with the structure of their catalytic sites, we measured and compared half-lives of unstable hydroxamic acids in the presence and absence of non-selective and selective esterase inhibitors (Figure 3 and Figures S1). We then calculated a score S for each esterase activity for a given hydroxamic acid and displayed results as

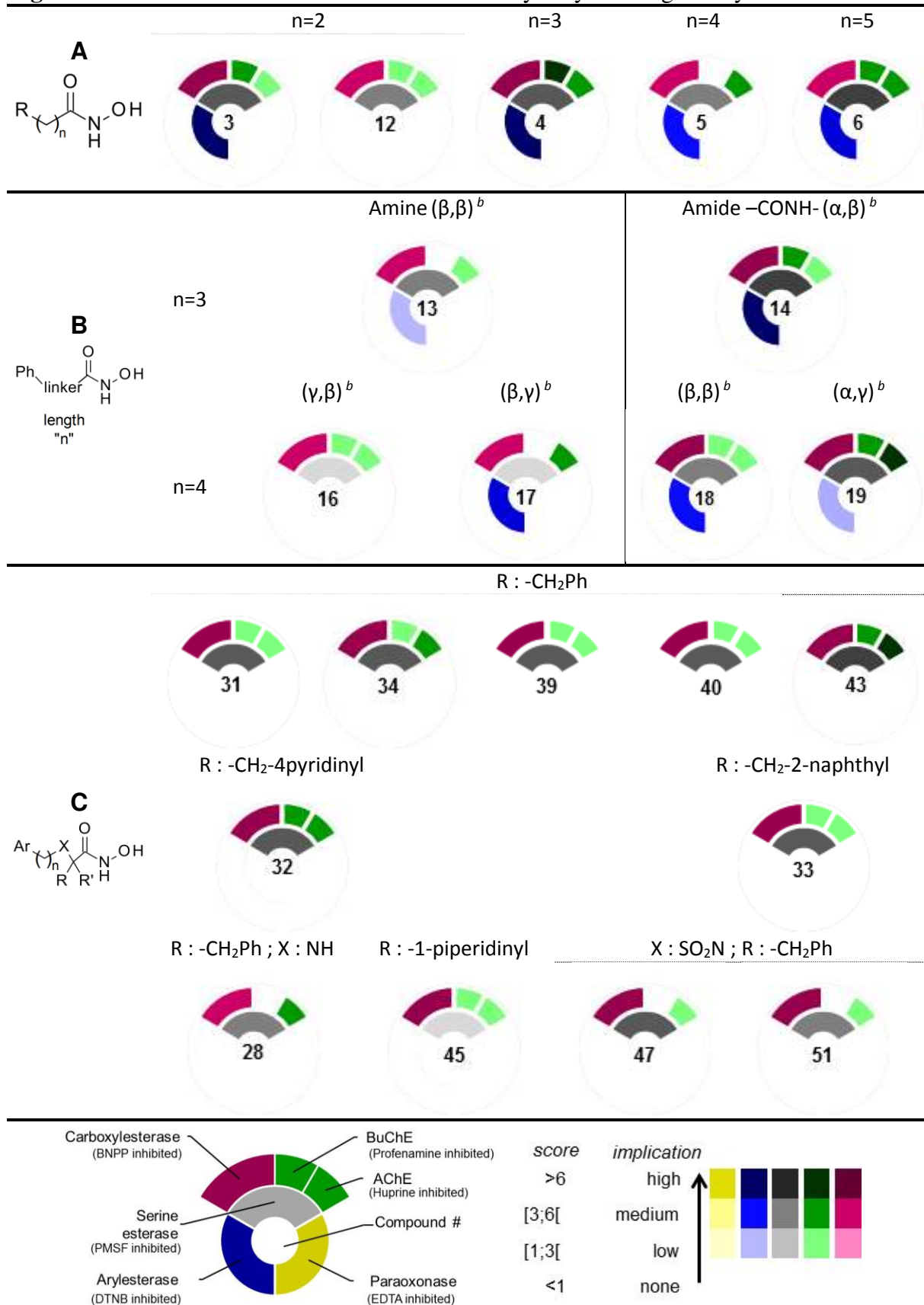
dashboards (Figure 4 and Supplementary methods) to provide a visual tool to compare the behavior of compounds in the light of the structure.

First, none of the hydroxamic acids is stabilized by the addition of EDTA to plasma, excluding paraoxonase from the set of hydroxamates hydrolyzing enzymes. Most linear analogues (A, B, Figure 4) that are unstable in plasma are usually stabilized by both DTNB (arylesterase inhibitor) and PMSF (serine esterase inhibitor), while branched hydroxamic acids (C, Figure 4) are not stabilized by DTNB.

In linear series, where the linker bears either methylene groups, amide groups or secondary amines, our study reveals implication of various esterases activities. In the first series (A), shorter chain lengths (≤ 3) are highly hydrolyzed by arylesterases and carboxylesterases (**3**, **4**) (Figure 4). Longer chains ($n = 4$ or 5) are moderately hydrolyzed by these enzymes (**5**, **6**) (Figure 4). Compound **12** is not stabilized by DTNB addition to plasma, in strong contrast with other linear hydroxamic acids, probably due to both bulkiness and lipophilicity of adamantyl group in comparison to phenyl (**12** vs **3**). Also, cholinesterases are only moderately implicated in the instability of these series. Interestingly, while BuChE is not involved in the hydrolysis of **5** ($n = 4$), it does participate in the instability of shorter compound **4** ($n = 3$) (Figure 4). Noteworthy, we were unable to stabilize hydroxamic acids **9** and **10**, both bearing a cyclohexyle side chain.

Introduction of a positive charge in β -position of the hydroxamic acid protects from hydrolysis by BuChE (**13** vs **3**) when chain length is 3 while, it protects from hydrolysis by arylesterases (**16** vs **5**) when chain length is 4. Conversely, introduction of a positive charge in γ -position of the hydroxamic acid, though improving stability, does not change the esterase activities implicated (**17** vs **5**).

Figure 4 : Involvement of esterase activities in the hydrolysis of a given hydroxamic acid.^a



^a Using score S calculated as given in Supplementary Methods. ^b Positions of the amine or the amide (from Ph-; from -CONHOH).

In the linear series, carboxylesterases seem more implicated in the hydrolysis of amide-containing compounds. Though no clear differences could be seen between **14**, **18** and **19**, no esterase inhibitor was able to stabilize related amide **21**, the reverse amide of **19**.

Substitution in α -position (C, Figure 4) prevents hydrolysis by arylerases while reinforcing hydrolysis by carboxylesterases. In malonic series (**31-34**, **39-40**, **43**), presence of a benzyl group, or 2-naphthyl-methyl or 4-pyridinyl-methyl analogues, results in similar susceptibility profiles. Interestingly, introduction of a positive charge (secondary amine) in β -position of the hydroxamic function reduces the involvement of BuChE as previously described in linear series (**28** vs **13** or **17**), while introduction of a positive charge (tertiary amine) in β -position (**45**) has no effect. This can be attributed to both steric constraints in **45** and to the absence of a benzyl substituent. At last, in sulfonamide series, generally quite stable, introduction of the benzyl group in α -position of the hydroxamic acid increased sensitivity to carboxylesterases, and AChE to a lesser extent.

Our study has also identified highly unstable hydroxamates **9**, **10**, **21** (Tables 2,3) for which no esterase inhibitor could restore stability in plasma. Co-incubation with a mixture of highly concentrated esterase inhibitors only slightly improves their half-lives by two-fold. We hypothesized that these hydroxamic acids were extremely affine substrates for esterases. To check this, we used them as competitors for other hydroxamic acids. For example, compound **4**, which displays an average half-life of 2 hours, is highly stabilized in the presence of either competitor **9**, **10** and **21** and its half-life is increased by 10-fold at least (Table 7 and Figure 5).

Table 7: Stabilization of 4.

competitor	$t_{1/2}$ (h) ^a
none	2.0
21	20.0
10	30.9
9	22.6

^a Half-life in rat plasma of **4** (10 μ M) in the absence or presence of competitor at 80 μ M.

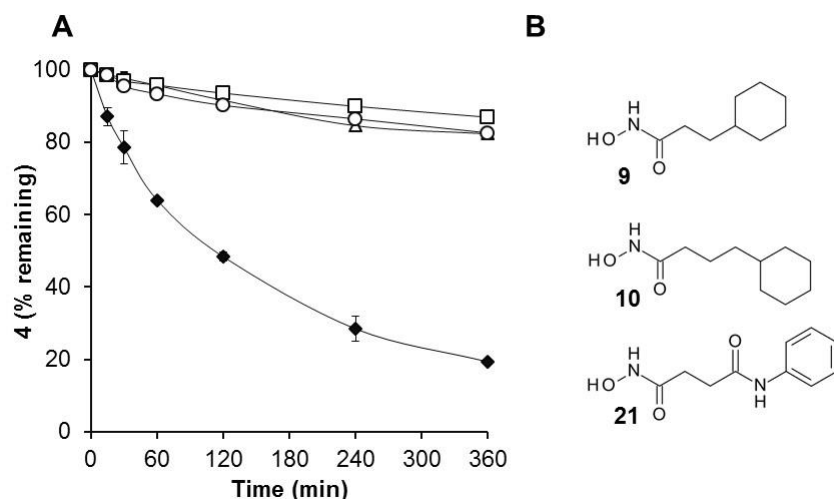


Figure 5 : Stabilization of **4** by highly unstable hydroxamic acids **9**, **10** and **21**.^a

^a % of **4** remaining in the absence (\blacklozenge) or presence of **9** (\circ), **10** (\square), **21** (\triangle).

As one of the AChE isoforms (isoform E) is found anchored to erythrocytes, we checked for stability of hydroxamic acids in whole blood. No significant differences between plasma and whole blood stabilities were observed. This suggests that this isoform does not contribute significantly to the hydrolysis of hydroxamates.

As well, outside the plasma compartment, two isoforms of carboxylesterases are present in liver (CES1) and intestine (CES2) microsomes. We therefore checked for stability of compound **3** on microsomes in non-oxidative conditions. **3** that displays a half-life of 0.8 h in plasma is also very unstable in liver microsomes ($t_{1/2} = 0.25$ h) while stable on intestine microsomes ($t_{1/2} > 6$ h). This result suggests an implication of CES1 rather than CES2, in the hydrolysis of this compound. This implication of CES1 was further confirmed by the fact that **3** is hydrolyzed by both rodent and human CES1 isolated enzymes, like several other hydroxamic acids (Supplementary Table S2).

To draw general trends, we compared Box and Whisker plots for each physical-chemical parameters (Supplementary Figures S9-11) for substrates and non substrates of ArE, AChE and CES. No differences were evidenced for AChE and CES substrates. On the contrary,

hydroxamic acids hydrolyzed by ArE display a cLogS and lower molecular weight and volume (Supplementary Figure S11). Because aryl esterase activity of plasma is not attributed to a specific enzyme, these results cannot be correlated with structural data.

Discussion

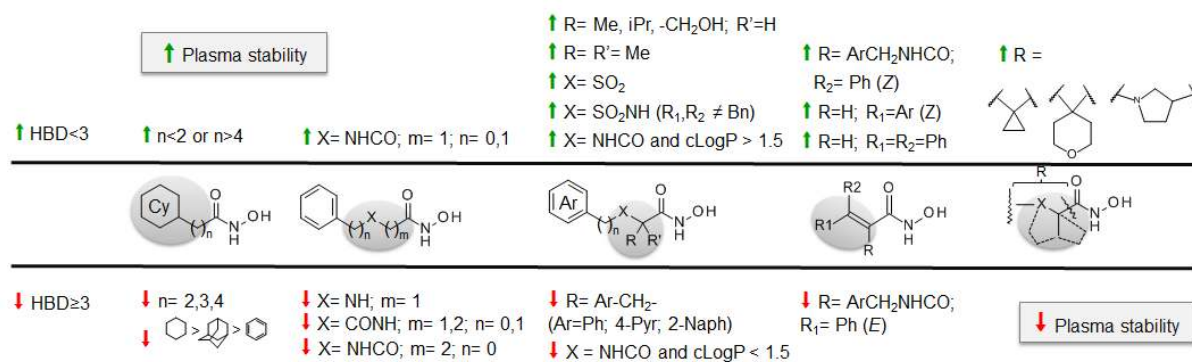


Figure 6 : Structure-Plasma Stability Relationships of hydroxamic acids: molecular properties and structural features increasing or decreasing stability.

Figure 6 summarizes Structure-Plasma Stability Relationships of hydroxamic acids. Regarding physical-chemical properties, HBD < 3 is beneficial for plasma stability. In the malonic series cLogP > 1.5 is deleterious for stability. Regarding structural features, combination of the nature or length of the linker with the hydrophobicity of the substituents is critical for stability. The presence of a tertiary carbon in α -position, in a cycle like cyclopropyle or tetrahydropyrane, stabilizes compounds. Also, bigger substituents like sulfonamides in β -position are usually beneficial for stability. Hydroxamic acids bearing a double bond in this study, proved to be stable towards esterase hydrolysis. Absence of an aryl-methyl substituent, either constrained or not, in α -position of the hydroxamic acid function, protects from hydrolysis.

CES recognize α -arylmethyl-substituted hydroxamic acids

CES is the prominent esterase involved in the hydrolysis of all unstable compounds (Figure 4). The preference of carboxylesterases for hydroxamic acids that display an aryl-

methyl group in α -position was rationalized by docking of **33**, **47**, **51** in a model of rat CES1 (Figure 7). Catalytic Ser221 points towards the carbonyl of the hydroxamic acid, with distances and angles compatible with the hydrolysis (Supplementary methods). Interestingly, the aryl-methyl group in α -position interacts nicely with Phe304 and Phe318. Moreover, Phe 318 position shifts in function of the size and distance of the aromatic group. For example, with the naphthyl analogue **33**, Phe 318 is pushed backwards, while for constrained analogue **51**, it moves closer (Figure 7). Interaction with these Phe side chains helps better positioning in front of the catalytic Ser. Consistently, docking of compounds less sensitive to CES-mediated hydrolysis showed that the hydroxamic carbonyls are further away from the catalytic Ser221 due to the lack of aryl-methyl group in α -position.

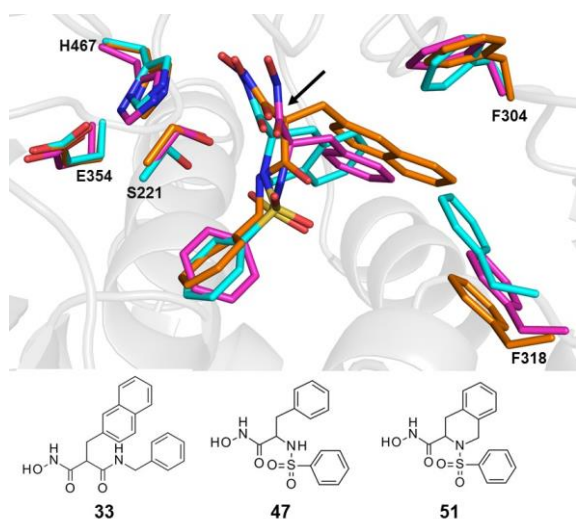


Figure 7 : Docking of 33, 47, 51 in rat CES1.^a

^a Carbon atoms for **33**, **47** and **51** and key residues in orange, magenta and cyan respectively. Arrow points carbonyl group of the hydroxamic function.

Shifting or inverting an amide dramatically impact stability.

To understand why compound **20** was stable while close amide analogues **18**, **19** and **21** were not (Table 3), these four compounds were docked in both mAChE and in rCES (Supplementary Figure S6-S7). For example, hydroxamic acid **18** is stabilized within mAChE pocket by hydrogen bonds between the carbonyl of the hydroxamic acid function and the oxyanion hole, a hydrogen bond with Ser125 and a H- π stacking to Tyr124. Similarly, the

carbonyl of the hydroxamic function of **21** interacts with the oxyanion hole. An additional hydrogen bond between its amide function and Glu202, via a water molecule, is observed in the model. In comparison with **18** and **21**, hydroxamic acid **19** makes fewer interactions with mAChE and the hydroxamic acid function is further away from the catalytic Ser203 (2.45 Å vs 2.24 Å for **18**, Supplementary Table S4). Finally, the stable hydroxamic acid **20**, does not appear to make significant interactions with the catalytic site of mAChE. As a consequence, the carbonyl of the hydroxamic acid function is too far to allow the attack by Ser203 (3.03 Å, Supplementary Figure S6 and Table S4). Similar results were obtained for rCES1 (Supplementary Figure S7). Binding of unstable hydroxamic acids **18** and **21** is driven by the interaction of the amide function with a water molecule in the vicinity of the oxyanion hole on one side, and π -stacking (parallel or T-shaped) with Phe304 and Phe318. Slightly more stable compound **19** is engaged in a H- π stacking with Leu255. In all these three cases, distances and angles to catalytic Ser221 are compatible with hydrolysis, in strong opposition with stable compound **20** (Supplementary Table S4). These results support the differences in stabilities for compounds **18-21** and corroborate the critical role of the amide position.

Plasma esterase activities differ between species.

All compounds of this study were shown to be stable in human plasma ($t_{1/2} > 6$ h) with the exception of compound **21**. This compound, though far more stable in human plasma ($t_{1/2} = 2.4$ h) than in rat plasma ($t_{1/2} = 0.43$ h), is still rapidly hydrolyzed in human plasma (Table 3). The greater stability of hydroxamates in human plasma compared to rat plasma can be explained by both structural differences in the catalytic pockets (Supplementary Figure S2-S5), and relative concentrations and activities of the esterases between species.

Regarding cholinesterases, hAChE and hBuChE catalytic pockets are narrower than that of rodent AChE and BuChE (Supplementary Figure S5) respectively. Importantly, there is only

a low concentration of AChE in human plasma, while BuChE is the most abundant esterase in human plasma⁴⁰.

We showed for a representative set of hydroxamic acids sensitive to CES hydrolysis that they are substrates of both rodent and human enzymes (Supplementary Table S2), in spite of structural differences in catalytic pockets (Supplementary Figure S5 E and F respectively). While CES are the main esterases involved in rat plasma hydrolysis of hydroxamic acids, the fact that CES are the most abundant esterases in rodent plasma while they are absent in human plasma, explains the difference of stabilities in rat and human plasma.⁴⁰ Moreover, because CES are present in liver and intestine microsomes, in both species, reducing the susceptibility of an hydroxamic acid to this enzyme is likely to have an impact on rodent plasma stability and human first-pass metabolism.

All the results obtained from this study can be used to guide the optimization of the plasma stability of hydroxamic acids. Some empirical rules are illustrated in Figure 8. For example, introduction of cyclic constrains, small α -substituents, removal or shortening of α -aryl-methyl groups improve stabilities, especially towards CES.

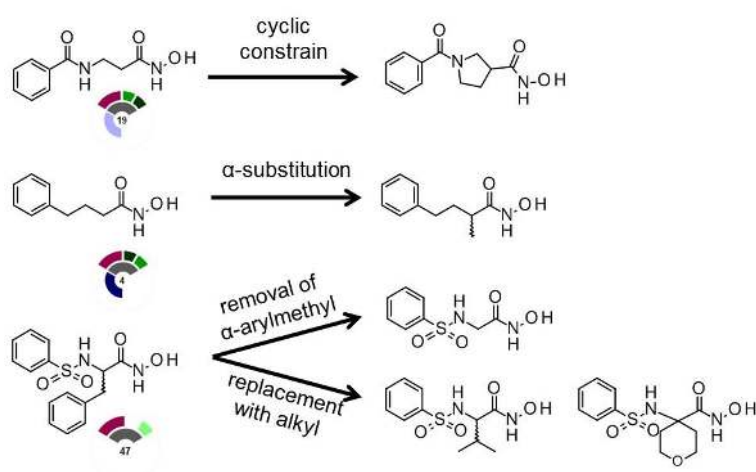


Figure 8 : Examples of the use of the medchem toolbox to stabilize hydroxamic acids.

Conclusion

We designed and synthesized a 57-member library of hydroxamic acids based on templates found in inhibitors of the main classes of Zinc metallohydrolases. This library was used to explore the Structure-Plasma Stability Relationships in chemical series relevant to the medicinal chemistry of this important class of therapeutic targets. In addition to including various chemical templates, the library covered a fair range of physical-chemical parameters (i.e. $137 < MW < 410$, $-1.4 < \log D < 3.4$, $49.3 < tPSA < 113$).

Finding 1: at the exception of one compound, all hydroxamates were found to be very stable in human plasma. In contrast, many hydroxamates were unstable in rat plasma. This difference between species may pose a difficulty during preclinical development, as it may preclude systemic exposure and engagement of target in species used in toxicological studies.

Finding 2: Thanks to a deconvolution scheme that uses a series of inhibitors of increasing selectivity, we were able to determine which enzyme was responsible for the hydrolysis.

It appears that hydrolysis of unstable hydroxamates is performed by a limited number of plasma enzymes, mainly CES.

Finding 3: This limited number of enzymes have defined structural requirements, in contrast with the large variety promiscuous metabolic enzymes such as CYP450 and phase 2 enzymes that account for the majority of transformations performed on xenobiotics. It was thus possible to identified structural features that are beneficial or deleterious for plasma stability. We identified for example that aryl-methyl substituent in α -position of the hydroxamic acid is well recognized by CES. Also, in linear amide-bearing compounds, the position and orientation of the amide bond relative to the hydroxamate is critical to recognition and stability: a NHCO in β -position of the hydroxamic function are stable while other amides are highly recognized by AChE and CES, leading to low stability. We also show that BuChE does not hydrolyze hydroxamic acids bearing a positive charge or bulky groups.

In term of molecular properties, we saw that stable hydroxamates are found in the low range of logP, while a systematic multivariate analysis yielded a model where HBD <3 favors stability (OR= 4.80).

As the hydroxamic acid function is often critical for the pharmacological activity, its replacement by isosters is often not possible. Also, stability in rodent plasma is essential to achieve proof-of-concept in animal, to assess secondary and safety pharmacology, and finally to estimate the safety window of drug candidates. Therefore a large difference in metabolic stability between human and preclinical species, especially when it involves transformation of a key element of pharmacophore can compromise developability of a drug candidate. Although the use of esterase inhibitors could partially restore adequate plasma concentration in animal models, these inhibitors have themselves side effects that could impede the interpretation of pharmacodynamic studies. In all, our study provides a toolbox that includes a validated protocol for hydroxamates stability testing, an esterase deconvolution procedure and SPSR that guide structural changes during optimization on the target of interest. It can help prioritizing hits and leads based on structural liabilities (templates and physical-chemical properties). This is the first comprehensive rule of thumb to obtain hydroxamic acids as stable in rodent as in human plasma, thus bridging the gap between species during preclinical development.

Experimental section

Chemistry.

General Chemistry. Merck Millipore aluminum-backed sheets TLC silica gel 60 F₂₅₄ were used for TLC. GraceResolv Cartridge columns (4 to 120 grams) were used to purify chemicals by flash column chromatography helped by Interchim Puriflash 430 equipped with evaporative light scattering detector (ELSD). ¹H and ¹³C NMR were recorded at room temperature on a Bruker DPX 300 at 300 and 75 MHz, respectively. ¹H NMR spectra chemical shifts are in parts per million (ppm) relative to the peak of DMSO-d₆ (2.50 ppm), CD₃OD (3.31 ppm), or CDCl₃ (7.26 ppm); ¹³C NMR spectra chemical shifts are in parts per million (ppm) relative to the peak of DMSO-d₆ (39.52 ± 0.06 ppm), CD₃OD (49.00 ± 0.06 ppm), acetone-d₆ (2.05 ± 0.06 ppm) or CDCl₃ (77.16 ± 0.06 ppm). Coupling constants (*J*) are reported in hertz (Hz) and peak multiplicities are reported as singlet (s), doublet (d), triplet (t), quadruplet (q), broad (br) and multiplet (m). Purity (%) was measured by reverse-phase chromatography HPLC using UV detection (215 nm) and all final compounds showed purities greater than 95%. Mass spectra were recorded on a LCMS system (Waters) composed of solvent manager 2695, photodiode array detector 2996, micromassZQ and a C₁₈ Xbridge 3.5µm particle size HPLC column, dimensions 4.6 x 50 mm. Analytical reverse phase HPLC gradient starting from 100% aqueous buffer pH = 3.8 ± 0.3 (NH₄OH 0.01%, HCOOH 0.02%) and reaching 100% acetonitrile buffer (NH₄OH 0.01%, HCOOH 0.02%) within 3.25min at a flow rate of 2 mL/min was used. When needed, compounds were purified by preparative HPLC on a LCMS Waters-2 system composed of solvent manager 2545, dual wavelength absorbance detector 2487, 3100 single quadrupole mass detector and using a Xbridge™ prep C₁₈ 5 µM OBD™ dimensions 50 mm x 250 mm column. Reverse phase preparative HPLC linear gradients started from 100% of aq. buffer pH = 3.8 ± 0.3 (NH₄OH 0.01%, HCOOH 0.02%) or aq. buffer pH = 9.2 ± 0.3 (NH₄OH 0.03%, HCOOH 0.01%) and reached corresponding 100% acetonitrile buffer (NH₄OH 0.01%,

HCOOH 0.02%) or (NH₄OH 0.03%, HCOOH 0.01%) within 25 min at a flow rate of 80 mL / min. High-resolution mass spectrometry (HRMS) was measured with a quadrupole time-of-flight (TOF) micromass Waters. Melting points were recorded on a Büchi melting point B-450. All commercial reagents and solvents were used without further purification. The synthesis of **37-38;40-42** has been previously described.^{8a;24}

Highly toxic compound. Potassium cyanide extracted in aqueous phase was stirred and basified with KOH 15% (pH has to be superior or equal to 14). Then sodium hypochlorite (NaClO) 2.6% active chloride was added in very large excess (compared to the amount of potassium cyanide) and stirred at room temperature for 10 min. Iodide strip was used to evaluate the oxidative potential of the mixture. A purple-blue color indicates a strong potential, allowing disposal of the treated phase in the adequate waste tank for destruction.

General procedure **A** for the synthesis of compounds **22b**, **24b-26b**, **29b**, **46b-47b**, **55b**. Ester (1.00 mmol, 1.0 equiv) was dissolved in ethanol/THF (1:2) and aqueous NaOH 2M (13.00 mmol, 13.0 equiv) was added. The solution was stirred at room temperature for 16 h. HCl 1 N was added to bring the pH up to 2-3. The resulting mixture was extracted with dichloromethane. The organic layer was dried over MgSO₄ and evaporated to give the corresponding carboxylic acid.

General procedure **B** for the synthesis of compounds **1-11**, **13-14**, **21-29**, **46-49**, **52-56**. Commercial carboxylic acid (2.00 mmol, 1 equiv) and HOBt (2.20 mmol, 1.1 equiv) were dissolved in DMF (10 mL). A solution of EDCI.HCl (2.70 mmol, 1.5 equiv) and *N*-methylmorpholine (6.01 mmol, 3 equiv) in DMF (6.5 mL) was slowly added to the previous solution cooled to 0 °C. Then a solution of *O*-tritylhydroxylamine (2.50 mmol, 1.25 equiv) in DMF (2.5 mL) was added. The mixture was stirred at room temperature overnight. The solvent was evaporated under reduced pressure and the residue was dissolved in DCM and washed two

times with aqueous sat. NaHCO_3 and two times with aqueous sat. NH_4Cl . The organic layer was dried over MgSO_4 , filtered and concentrated under reduced pressure to give the desired *O*-tritylhydroxamic acid. The corresponding *O*-tritylhydroxamic acid (1 mmol, 1 equiv) was dissolved in DCM (9.50 mL) and liquid TFA (0.25 mL) and triethylsilane (0.25 mL) were added. The mixture was stirred at room temperature for 30 min. Solvents were removed under reduced pressure and the crude product was washed three times with pentane/diethyl ether 75:25 (v:v) affording a residue. The corresponding residue was purified by preparative HPLC using a linear acetonitrile/water (ammonium acetate/formic acid buffer, pH = 3.8) gradient (2:98 to 100:0 over 25min), for hydroxamic acids **3-4, 9-10, 14**. Or the residue was washed with diethyl ether/petroleum ether (1:4) to give a crude product which was purified by flash silica gel column chromatography to give desired hydroxamic acid **1-2, 5-8, 11, 13, 21-29, 46-49, 52-56**.

General procedure C, for the synthesis compounds **30-32, 34-36, 39, 43**. To a solution of diethyl 2-methylmalonate (3.56 mmol, 1 equiv) in ethanol absolute (5 mL, 0.7 M) was added solid KOH (5.34 mmol, 1.5 equiv). This mixture was stirred for 24 h at room temperature before EtOH was evaporated *in vacuo*. The residue was dissolved in aqueous sat. NaHCO_3 and washed with EtOAc. The aqueous phase was acidified to pH 1-2 with aqueous HCl 1M. The desired carboxylic acid was extracted thrice with ethyl acetate, organic phases were pooled and evaporated to give pure carboxylic acid **63-68**. To a solution of the appropriate carboxylic acid (2.70 mmol, 1 equiv) in anhydrous DMF (6.60 mL, 0.5 M) at 0 °C were added HBTU (2.97 mmol, 1.1 equiv) and anhydrous DIPEA (8.1 mmol, 3 equiv). This mixture was stirred 5 min before benzylamine (2.83 mmol, 1.05 equiv) was added. The mixture was stirred 10 min at 0 °C, and 4h30 at room temperature. The solvent was evaporated under high vacuum and the crude product was partitioned between aqueous sat. NaHCO_3 and EtOAc. The organic layer

was washed 3 times with aqueous sat. NaHCO₃, dried over MgSO₄ and evaporated under vacuum. The residue was purified by flash silica gel column chromatography (cyclohexane/EtOAc 1:0 to 1:1 (v:v)), affording the corresponding ethyl 2-(benzylcarbamoyl)-2-methylacetate **30a-32a**, **34a-36a**, **39a**, **43a**. To a solution of the latter (1.94 mmol, 1 equiv) in MeOH (4.31 mL, 0.45 M) was added a solution of aqueous hydroxylamine 50% (4.31 mL) and KCN (0.012 g, 0.019 mmol, 0.1 equiv). The mixture was stirred 15 h 30 min at room temperature before it was concentrated under vacuum. The residue was partitioned between water and EtOAc (1:50, v:v). The organic layer was evaporated under vacuum and purified by preparative HPLC using a linear acetonitrile/water (ammonium-acetate/formic acid buffer, pH = 3.8) gradient, (2:98 to 100:0 over 25min). This afforded pure hydroxamic acids **30-32**, **34-36**, **39**, **43**.

Benzhydroxamic acid (1). Obtained following the general procedure **B** from benzoic acid. White solid (0.075 g, 17%). Purity: 98%. mp: 129 °C. $t_{R,LCMS} = 1.37$ min. MS (ESI⁻): $m/z = 136$ [M-H]⁻, MS (ESI⁺): $m/z = 138$ [M+H]⁺. ¹H NMR 300 MHz (DMSO-*d*₆) δ (ppm): 11.19 (s, 1H), 9.02 (s, 1H), 7.74 (dd, $J = 1.5$ Hz, $J = 7.5$ Hz, 2H), 7.53-7.41 (m, 3H). ¹³C NMR 75 MHz (DMSO-*d*₆) δ (ppm): 164.1, 132.8, 131.1, 128.3, 126.8. HRMS m/z calculated for C₇H₈NO₂ [M+H]⁺: 138.0555. Found: 138.0566.

2-Phenylethanehydroxamic acid (2). Obtained following the general procedure **B** from 2-phenylacetic acid. Light brown solid (0.063 g, 13%). Purity: 96%. mp: 119 °C. $t_{R,LCMS} = 1.52$ min. MS (ESI⁻): $m/z = 150$ [M-H]⁻, MS (ESI⁺): $m/z = 152$ [M+H]⁺. ¹H NMR 300 MHz (DMSO-*d*₆) δ (ppm): 10.65 (s, 1H), 8.81 (s, 1H), 7.32-7.19 (m, 5H), 3.27 (s, 2H). ¹³C NMR 75 MHz (DMSO-*d*₆) δ (ppm): 167.0, 136.0, 129.3, 128.9, 128.1, 126.4, 39.4. HRMS m/z calculated for C₈H₁₀NO₂ [M+H]⁺: 152.0712. Found: 152.0734.

3-Phenylpropanehydroxamic acid (3). Obtained following the general procedure **B**. White solid (0.084 g, 26%). Purity 98%. mp: 80 °C. $t_{R,LCMS} = 1.76$ min. MS (ESI-): $m/z = 164$ [M-H]⁻, MS (ESI+): $m/z = 166$ [M+H]⁺. ¹H NMR 300 MHz (CDCl₃) δ (ppm): 10.35 (s, 1H), 8.70 (s, 1H), 7.29-7.14 (m, 5H), 2.82-2.78 (t, $J = 7.5$ Hz, 2H), 2.27-2.22 (t, $J = 7.5$ Hz, 2H). ¹³C NMR 75 MHz (CDCl₃) δ (ppm): 171.1, 140.3, 128.8, 128.4, 126.7, 34.9, 31.5. HRMS m/z calculated for C₉H₁₂NO₂ [M+H]⁺: 166.0868. Found: 166.0882.

4-Phenylbutanehydroxamic acid (4). Obtained following the general procedure **B**. Brown oil (0.176 g, 51%). Purity 95%. $t_{R,LCMS} = 1.94$ min. MS (ESI-): $m/z = 178$ [M-H]⁻, MS (ESI+): $m/z = 180$ [M+H]⁺. ¹H NMR 300 MHz (DMSO-*d*₆) δ (ppm): 10.36 (s, 1H), 8.69 (br s, 1H), 7.31-7.15 (m, 5H), 2.57-2.55 (t, $J = 7.5$ Hz, 2H), 1.99-1.94 (t, $J = 7.5$ Hz, 2H), 1.83-1.73 (m, 2H). ¹³C NMR 75 MHz (DMSO-*d*₆) δ (ppm): 169.1, 141.9, 128.5, 126.0, 34.8, 32.0, 27.2. HRMS m/z calculated for C₁₀H₁₄NO₂ [M+H]⁺: 180.1025. Found: 180.1049.

5-Phenylpentanehydroxamic acid (5). Obtained following the general procedure **B** from 5-phenylpentanoic acid. White solid (0.036 g, 10%). Purity: 90%. mp: 74 °C. $t_{R,LCMS} = 2.47$ min. MS (ESI+): $m/z = 194$ [M+H]⁺. ¹H NMR 300 MHz (acetone-*d*₆) δ (ppm): 7.27-7.12 (m, 2H), 2.61-2.57 (m, 2H), 2.15-2.10 (m, 2H), 2.08-2.03 (m, 2H), 1.70-1.59 (m, 4H). ¹³C NMR 75 MHz (acetone-*d*₆) δ (ppm): 170.2, 142.3, 128.3, 128.2, 125.6, 35.2, 30.9, 25.0. HRMS m/z calculated for C₁₁H₁₆NO₂ [M+H]⁺: 194.1181. Found: 194.1180.

6-Phenylhexanehydroxamic acid (6). Obtained following the general procedure **B** from 6-phenylhexanoic acid. White solid (0.247 g, 45%). Purity: 99%. mp: 71 °C. $t_{R,LCMS} = 2.72$ min. MS (ESI+): $m/z = 208$ [M+H]⁺. ¹H NMR 300 MHz (DMSO-*d*₆) δ (ppm): 10.31 (br s, 1H), 10.00

(br s, 1H), 8.64 (br s, 1H), 7.28-7.13 (m, 5H), 2.57-2.49 (m, 7H), 1.92 (t, $J = 14.4$ Hz, 2H), 1.59-1.51 (m, 4H), 1.29-1.27 (m, 2H). ^{13}C NMR 75 MHz (DMSO- d_6) δ (ppm): 169.5, 142.7, 128.7, 128.7, 126.1, 35.5, 32.7, 31.2, 28.7, 25.4. HRMS m/z calculated for $\text{C}_{12}\text{H}_{18}\text{NO}_2$ $[\text{M}+\text{H}]^+$: 208.1338. Found: 208.1334.

7-Phenylheptanehydroxamic acid (7). Obtained following the general procedure **B** from 7-phenylheptanoic acid. White powder (0.060 g, 13%). Purity 96%. mp: 66 °C. $t_{\text{R,LCMS}} = 2.97$ min. MS (ESI+): $m/z = 222$ $[\text{M}+\text{H}]^+$. ^1H NMR 300 MHz (acetone- d_6) δ (ppm): 7.27-7.11 (m, 5H), 2.58 (t, $J = 7.5$ Hz, 2H), 2.09 (t, $J = 7.5$ Hz, 2H), 1.62-1.55 (m, 4H), 1.34-1.29 (m, 4H). ^{13}C NMR 75 MHz (acetone- d_6) δ (ppm): 170.3, 142.6, 128.3, 128.2, 125.5, 35.5, 32.3, 31.3, 29.0, 25.3. HRMS m/z calculated for $\text{C}_{13}\text{H}_{20}\text{NO}_2$ $[\text{M}+\text{H}]^+$: 222.1494. Found: 222.1494.

2-Cyclohexylethanehydroxamic acid (8). Obtained following the general procedure **B** from 2-cyclohexylacetic acid. White solid (0.107g, 18%). Purity: 80%. mp: 146 °C. $t_{\text{R,LCMS}} = 2.20$ min. MS (ESI+): $m/z = 158$ $[\text{M}+\text{H}]^+$. ^1H NMR 300 MHz (DMSO- d_6) δ (ppm): 10.31 (br s, 1H), 8.64 (br s, 1H), 1.81 (d, $J = 6.3$ Hz, 2H), 1.62 (d, $J = 7.5$ Hz, 6H), 1.20-1.06 (m, 3H), 0.92-0.85 (m, 2H). ^{13}C NMR 75 MHz (DMSO- d_6) δ (ppm): 168.6, 40.8, 34.9, 32.9, 26.3, 26.0. HRMS m/z calculated for $\text{C}_8\text{H}_{16}\text{NO}_2$ $[\text{M}+\text{H}]^+$: 158.1181. Found: 158.1179.

3-Cyclohexylpropanehydroxamic acid (9). Obtained following the general procedure **B**. Colorless oil (0.072 g, 21%). Purity 99%. $t_{\text{R,LCMS}} = 2.49$ min. MS (ESI-): $m/z = 170$ $[\text{M}-\text{H}]^-$, MS (ESI+): $m/z = 172$ $[\text{M}+\text{H}]^+$. ^1H NMR 300 MHz (DMSO- d_6) δ (ppm): 1.96-1.91 (t, $J = 7.5$ Hz, 2H), 1.67-1.63 (m, 5H), 1.41-1.33 (m, 2H), 1.23-1.08 (m, 4H), 0.88-0.78 (q, $J = 10.2$ Hz, 2H). ^{13}C NMR 75 MHz (DMSO- d_6) δ (ppm): 169.3, 36.5, 32.6, 32.5, 29.8, 26.1, 25.7. HRMS m/z calculated for $\text{C}_9\text{H}_{18}\text{NO}_2$ $[\text{M}+\text{H}]^+$: 172.1338. Found: 172.1354.

4-Cyclohexylbutanehydroxamic acid (10). Obtained following the general procedure **B**. White solid (0.034 g, 9%). Purity 98%. mp: 81 °C. $t_{R,LCMS} = 2.42$ min. MS (ESI⁻): $m/z = 184$ [M-H]⁻, MS (ESI⁺): $m/z = 186$ [M+H]⁺. ¹H NMR 300 MHz (DMSO-*d*₆) δ (ppm): 10.28 (br s, 1H), 8.63 (br s, 1H), 1.89 (t, $J = 7.5$ Hz, 2H), 1.66-1.62 (m, 5H), 1.53-1.42 (quin, $J = 7.5$ Hz, 2H), 1.24-1.06 (m, 6H), 0.88-0.77 (m, 2H). ¹³C NMR 75 MHz (DMSO-*d*₆) δ (ppm): 169.1, 36.8, 36.4, 32.8, 32.5, 26.2, 25.8, 22.5. HRMS m/z calculated for C₁₀H₂₀NO₂ [M+H]⁺: 186.1494. Found: 186.1517.

2-(1-Adamantyl)ethanehydroxamic acid (11). Obtained following the general procedure **B** from 2-(adamantan-1-yl)acetic acid. White solid (0.120 g, 48%). Purity 99%. mp: 173 °C. $t_{R,LCMS} = 2.63$ min. MS (ESI⁺): $m/z = 210$ [M+H]⁺. ¹H NMR 300 MHz (DMSO-*d*₆) δ (ppm): 10.20 (br s, 1H), 1.90 (s, 3H), 1.68-1.54 (m, 14H). ¹³C NMR 75 MHz (DMSO-*d*₆) δ (ppm): 167.2, 47.1, 42.5, 36.9, 32.6, 28.5. HRMS m/z calculated for C₁₂H₂₀NO₂ [M+H]⁺: 210.1494. Found: 210.1507.

3-(1-Adamantyl)propanehydroxamic acid (12). To a solution of 2-(1-adamantyl)ethanol (1.984 g, 11 mmol, 1 equiv) in pyridine (13.7 mL, 0.8 M) was added 4-methylbenzenesulfonyl chloride (2.098 g, 11 mmol, 1 equiv) and the resulting yellow mixture was stirred 20 h at room temperature. Pyridine was evaporated under vacuum and the crude product was dissolved in EtOAc. The organic phase was washed twice with 1 N HCl then twice with aqueous sat. NaHCO₃, dried over MgSO₄, filtered and concentrated to afford 2-(1-adamantyl)ethyl 4-methylbenzenesulfonate (3.003 g, 75%) as a colorless oil. Purity 91%. $t_{R,LCMS} = 3.95$ min. MS (ESI⁺): $m/z = 357$ [M+Na]⁺. ¹H NMR 300 MHz (DMSO-*d*₆) δ (ppm): 7.79 (d, $J = 8.3$ Hz, 2H), 7.48 (d, $J = 8.3$ Hz, 2H), 4.05 (t, $J = 6.9$ Hz, 2H), 2.42 (s, 3H), 1.85 (s, 3H), 1.63-1.49 (m, 8H),

1.37-1.33 (m, 8H). ^{13}C NMR 75 MHz (DMSO- d_6) δ (ppm): 144.8, 132.4, 130.1, 127.6, 67.4, 41.8, 41.5, 36.3, 31.2, 27.8, 21.0. To a solution of this tosylate (2.342 g, 7.00 mmol, 1 equiv) in DMF (8.75 mL, 0.8 M) was added KCN (0.911 g, 14.00 mmol, 2 equiv). The resulting suspension was stirred at 80 °C for 15 h. It was diluted with water and extracted with Et₂O. The combined organic phases were washed with water and brine, dried over MgSO₄ and concentrated *in vacuo* to give 1.126 g of a yellow oil. This crude product was purified by flash silica gel column chromatography (cyclohexane/ethyl acetate, 90:10 to 70:30). Pure 3-(1-adamantyl)propanenitrile **58** (1.126 g, 84%) was obtained as yellow needle crystals. No signal by LCMS. ^1H NMR 300 MHz (DMSO- d_6) δ (ppm): 2.40 (t, J = 8.0 Hz, 2H), 1.92 (br s, 3H), 1.62 (br q, J = 12.3 Hz, 6H), 1.44 (d, J = 2.5 Hz, 6H), 1.36 (t, J = 8.0 Hz, 3H). ^{13}C NMR 75 MHz (DMSO- d_6) δ (ppm): 121.6, 40.9, 36.6, 31.7, 27.8, 10.2. To a solution of **58** (0.869 g, 4.59 mmol, 1 equiv) in EtOH (9.20 mL, 0.5 M) was added a solution of KOH (0.901 g, 16.07 mmol, 3.5 equiv) in H₂O (9.20 mL, 1.75 M). The mixture was heated to 90 °C for 20 h. Solvents were evaporated *in vacuo* then the residue was dissolved in aqueous HCl 1M and EtOAc. The organic phase was washed three times with HCl 1M, once with brine and dried over MgSO₄. EtOAc was evaporated *in vacuo* affording 3-(1-adamantyl)propanoic acid (0.942 g, 97%) as white crystals. TLC cyclohexane/EtOAc 70:30 (v:v) R_f = 0.5. To a solution of this acid (0.309 g, 1.48 mmol, 1 equiv) in anhydrous methanol (5 mL, 0.33 M) cooled to 0 °C was added dropwise thionyl chloride (0.323 mL, 4.45 mmol, 3 equiv). The reaction was stirred at room temperature for 4 h 30 min before solvents were evaporated under vacuum. White crystals were obtained which were dissolved in EtOAc (a white precipitate appear) and washed with aqueous NaHCO₃ 5% (The white precipitate disappear when aqueous phase was added). The crude product methyl 3-(1-adamantyl)propanoate **12a** was obtained as a white powder (0.071 g, 21%) by evaporating the solvent and was used in the next step without further purification. TLC cyclohexane/EtOAc 70:30 (v:v) R_f = 0.90. To a solution of **12a** (0.071 g, 0.31 mmol, 1 equiv) in MeOH (0.700 mL,

0.45 M) was added a solution of aqueous hydroxylamine 50% (0.700 mL) before KCN (0.02 g, 0.028 mmol, 0.1 equiv). The mixture was stirred 12 h 30 min at room temperature. It was concentrated under vacuum and an aqueous workup was performed using H₂O/EtOAc (1:50 (v:v)). The organic layer was evaporated under vacuum and purified by preparative HPLC using a linear acetonitrile/water (ammonium-acetate/formic acid buffer, pH = 9.2) gradient (2:98 to 100:0 over 25min) affording 3-(1-adamantyl)propanehydroxamic acid **12** as a white powder (0.026 g, 36%). Purity 99%. mp: 153 °C. TLC cyclohexane/EtOAc 70:30 (v:v) R_f = 0.50. t_{R,LCMS} = 2.57 min. MS (ESI-) : m/z = 222 [M-H]⁻, MS (ESI+): m/z = 224 [M+H]⁺. ¹H NMR 300 MHz (CD₃OD-*d*₄) δ (ppm): 10.31 (s, 1H), 8.62 (d, *J* = 1.2 Hz, 1H), 1.91-1.85 (m, 5H), 1.61 (q, *J* = 12.1 Hz, 6H), 1.41 (d, *J* = 2.1 Hz, 6H), 1.25 (td, *J* = 5.4 Hz, *J* = 2.8 Hz, 2H). ¹³C NMR 75 MHz (CD₃OD-*d*₄) δ (ppm): 169.8, 41.5, 36.5, 31.6, 27.9, 26.0. HRMS m/z calculated for C₁₃H₂₂NO₂ [M+H]⁺: 224.1651. Found: 224.1664.

2-(Benzylamino)ethanehydroxamic acid (13). Obtained following the general procedure **B** from N-benzylglycine hydrochloride. White powder (0.070 g, 25%). Purity 99%. mp: 169 °C. t_{R,LCMS} = 1.47 min. MS (ESI+): m/z = 181 [M+H]⁺. ¹H NMR 300 MHz (DMSO-*d*₆) δ (ppm): 10.94 (br s, 1H), 9.31 (br s, 1H), 9.26 (br s, 1H), 7.45-7.42 (m, 5H), 4.16 (s, 2H), 3.55 (s, 2H). ¹³C NMR 75 MHz (DMSO-*d*₆) δ (ppm): 162.2, 131.9, 130.5, 129.5, 129.2, 50.4, 45.2. HRMS m/z calculated for C₉H₁₃N₂O₂ [M+H]⁺: 181.0972. Found: 181.0977.

N-[2-(Hydroxyamino)-2-oxo-ethyl]benzamide (14). Obtained following the general procedure **B**. White solid (0.008 g, 5%). Purity 97%. mp: 149 °C. t_{R,LCMS} = 1.43 min. MS (ESI-): m/z = 193 [M-H]⁻, MS (ESI+): m/z = 195 [M+H]⁺. ¹H NMR 300 MHz (CD₃OD-*d*₄) δ (ppm): 7.88-7.85 (dd, *J* = 0.9 Hz, *J* = 8.1 Hz, 2H), 7.54 (tt, *J* = 0.9 Hz, *J* = 7.5 Hz, 1H), 7.46 (td, *J* = 7.5 Hz, *J* = 8.1 Hz, 2H), 3.99 (s, 2H). ¹³C NMR 75 MHz (CD₃OD-*d*₄) δ (ppm): 170.7, 169.1, 135.2,

133.1, 129.8, 128.7, 42.1. HRMS m/z calculated for $C_9H_{11}N_2O_3$ $[M+H]^+$: 195.0770. Found: 195.0799.

3-(Hydroxyamino)-3-oxo-N-phenyl-propanamide (**15**). A solution of commercial Meldrum's acid (0.332 g, 2.30 mmol, 1 equiv) and aniline (0.631 mL, 6.91 mmol, 3 equiv) in MeCN (1.85 mL, 1.25 M) was stirred for 2 h at 80 °C. The mixture was evaporated under vacuum and the residue was partitioned between aqueous sat. $NaHCO_3$ and EtOAc. The aqueous phase was acidified to pH 1-2 with HCl 1M and extracted with ethyl acetate. Solvents were evaporated under reduced pressure to afford 3-anilino-3-oxo-propanoic acid **15b** (0.202 g, 48%) as white crystals. $t_{R,LCMS} = 1.60$ min. MS (ESI-): $m/z = 178$ $[M-H]^-$, MS (ESI+): $m/z = 180$ $[M+H]^+$. Caution: a 40% rate of degradation was observed after 3 days at room temperature (brown color appears on crystals). Impure carboxylic acid **15b** (0.202 g, 1.12 mmol, 1 equiv) was solubilized in anhydrous MeOH (3.5 mL, 0.32 M) at 0 °C. $SOCl_2$ (0.246 mL, 3.38 mmol, 3 equiv) was added dropwise and the mixture was stirred for 1 h at room temperature. The mixture was dissolved in EtOAc (10 mL) and water (20 mL). The aqueous phase was extracted twice with EtOAc, organic phases were pooled, dried over $MgSO_4$ and evaporated under vacuum, affording Methyl 3-anilino-3-oxo-propanoate **15a** as a white powder (0.189 g, 43%) with a purity of only 50%. **15a** was anyway used in the final step without further purification. $t_{R,LCMS} = 2.02$ min. MS (ESI-): $m/z = 192$ $[M-H]^-$, MS (ESI+): $m/z = 194$ $[M+H]^+$. To a solution of **15a** (0.189 g, 0.98 mmol, 1 equiv) in MeOH (4 mL, 0.25 M) was added a solution of aqueous hydroxylamine 50% (4 mL,) and KCN (0.032 g, 0.49 mmol, 0.5 equiv). The solution was stirred overnight at room temperature. It was concentrated under vacuum and an aqueous workup was performed using $H_2O/EtOAc$ (1:50 (v:v)). The organic layer was evaporated under vacuum and purified by preparative HPLC using a linear acetonitrile/water (ammonium-acetate/formic acid buffer, pH = 3.8) gradient (2:98 to 100:0 over 25 min), affording the

hydroxamic acid **15** as a white powder (0.015 g, 8%). Purity 96%. mp: 149 °C. $t_{R,LCMS}$ = 1.55 min. MS (ESI-): m/z = 193 [M-H]⁻, MS (ESI+): m/z = 195 [M+H]⁺. ¹H NMR 300 MHz (DMSO-*d*₆) δ (ppm): 10.10 (s, 1H), 7.59-7.56 (m, 2H), 7.30 (t, J = 7.4 Hz, 2H), 7.04 (t, J = 7.4 Hz, 1H), 3.11 (s, 2H). ¹³C NMR 75 MHz (DMSO-*d*₆) δ (ppm): 165.5, 163.6, 138.9, 128.7, 123.4, 119.0, 42.0. HRMS m/z calculated for C₉H₁₁N₂O₃ [M+H]⁺: 195.0770. Found: 195.0801.

2-(2-Phenylethylamino)ethanehydroxamic acid (16). To a solution of 2-phenylethanamine (0.162 g, 1.33 mmol, 1 equiv) and anhydrous DIPEA (0.244 mL, 1.40 mmol, 1.05 equiv) in anhydrous DMF (2.40 mL, 0.55 M) at 0 °C was added dropwise methyl 2-bromoacetate (0.123 mL, 1.33 mmol, 1 equiv). The mixture was stirred for 1 h at 0 °C and 3 h at room temperature. Solvents were evaporated *in vacuo* and the brown crude product was purified by flash silica gel column chromatography (cyclohexane/EtOAc, 100:0 to 30:70) affording methyl 2-(2-phenylethylamino)acetate (**16a**) as a colorless oil (0.146 g, 54%). $t_{R,LCMS}$ = 1.65 min. MS (ESI+): m/z = 194 [M+H]⁺. To a solution of **16a** (0.086 g, 0.44 mmol, 1 equiv) in MeOH (0.490 mL; 0.45 M) was added a solution of aqueous hydroxylamine 50% (4.90 mL) and KCN (0.003 g, 0.05 mmol, 0.1 equiv). The mixture was stirred for 3 h 30 min at room temperature. It was concentrated under vacuum and an aqueous workup was performed using H₂O/EtOAc (1:50 (v:v)). The organic layer was evaporated under vacuum and purified by preparative HPLC using a linear acetonitrile/water (ammonium-acetate/formic acid buffer pH = 9.2) gradient (2:98 to 100:0 over 25 min), affording the hydroxamic acid **16** as a white powder (0.032 g, 36%). Purity 98%. mp: 146 °C. $t_{R,LCMS}$ = 1.47 min. MS (ESI-): m/z = 193 [M-H]⁻, MS (ESI+): m/z = 195 [M+H]⁺. ¹H NMR 300 MHz (DMSO-*d*₆) δ (ppm): 7.30-7.14 (m, 5H), 3.03 (s, 2H), 2.68 (s, 4H). ¹³C NMR 75 MHz (DMSO-*d*₆) δ (ppm): 167.8, 140.2, 128.5, 128.2, 125.8, 50.5, 49.8, 35.7. HRMS m/z calculated for C₁₀H₁₅N₂O₂ [M+H]⁺: 195.1134. Found: 195.1140.

3-(Benzylamino)propanehydroxamic acid (17). To a solution of methyl prop-2-enoate (0.316 mL, 3.48 mmol, 1 equiv) in ethanol (1.70 mL, 2 M) was added benzylamine (0.381 mL, 3.48 mmol, 1 equiv) and the mixture was stirred for 18 h at room temperature. The crude product was purified by flash silica gel column chromatography (DCM/MeOH, 100:0 to 90:10) affording methyl 3-(benzylamino)propanoate **17a** (0.603 g, 84%) as a colorless oil. Purity 94%. $t_{R,LCMS} = 1.47$ min. MS (ESI+): $m/z = 194$ [M+H]⁺. To a solution of **17a** (0.603 g, 3.12 mmol, 1 equiv) in methanol (6.80 mL, 0.45 M) was added a solution of aqueous hydroxylamine 50% (6.80 mL) and KCN (0.02 g, 0.28 mmol, 0.1 equiv). The mixture was stirred for 3 h 30 min at room temperature. It was then concentrated under vacuum and an aqueous workup was performed using H₂O/EtOAc (1:50 (v:v)). The organic layer was evaporated under vacuum and purified by flash column chromatography (DCM/MeOH, 100:0 to 85:15) affording the hydroxamic acid **17** as white crystals (0.097 g, 15%). Purity 99%. mp: 118 °C. $t_{R,LCMS} = 1.17$ min. MS (ESI-): $m/z = 193$ [M-H]⁻, MS (ESI+): $m/z = 195$ [M+H]⁺. ¹H NMR 300 MHz (DMSO-*d*₆) δ (ppm): 7.30 (m, 4H), 7.22 (m, 1H), 3.66 (s, 2H), 2.67 (t, *J* = 6.9 Hz, 2H), 2.12 (t, *J* = 6.9 Hz, 2H). ¹³C NMR 75 MHz (DMSO-*d*₆) δ (ppm): 168.3, 140.8, 128.1, 127.9, 126.5, 52.7, 45.0, 33.0. HRMS m/z calculated for C₁₀H₁₅N₂O₂ [M+H]⁺: 195.1134. Found: 195.1140.

N-Hydroxycarbamoylmethyl-2-phenyl-acetamide (18). To a solution of hydroxylamine hydrochloride (2.12 g, 30.57 mmol, 7 equiv) in MeOH (35 mL) was added KOH (2.70 g, 48.0 mmol, 11 equiv). The mixture was stirred 30 min at room temperature. This solution was then filtered and added to a solution of methyl 2-(2-phenylacetamido)acetate **18a** (0.905 g, 4.37 mmol, 1 equiv) in MeOH (25 mL). The mixture was stirred at room temperature for 16 h. Solvent was removed under reduced pressure. The residue was dissolved in H₂O, acidified to pH = 5 with 6 N HCl, and neutralized with aqueous sat. NaHCO₃. Precipitate was collected by filtration to give compound **18** as a pasty amorphous solid. Purity 99%. $t_{R,LCMS} = 1.53$ min. MS

(ESI-): $m/z = 207$ [M-H]⁻. ¹H NMR 300 MHz (CD₃OD-*d*₄) δ (ppm): 7.31-7.23 (m, 5H), 3.74 (s, 2H), 3.55 (s, 2H). ¹³C NMR 75 MHz (DMSO-*d*₆) δ (ppm): 170.3, 165.3, 138.5, 129.6, 128.4, 126.2, 44.4, 40.3. HRMS m/z calculated for C₁₀H₁₃N₂O₃ [M+H]⁺: 209.0926. Found: 209.0917.

N-[3-(Hydroxyamino)-3-oxo-propyl]benzamide (**19**). To a solution of methyl 3-benzamidopropanoate (0.123 g, 0.59 mmol, 1 equiv) in MeOH (1.60 mL, 0.45 M) was added a solution of aqueous hydroxylamine 50% (1.30 mL) and KCN (0.004 g, 0.05 mmol, 0.1 equiv). The mixture was stirred for 2 h 15 min at room temperature. It was then concentrated under vacuum and an aqueous workup was performed using H₂O/EtOAc (1:50 (v:v)). The organic layer was evaporated under vacuum and purified by preparative HPLC using a linear acetonitrile/water (ammonium-acetate/formic acid buffer, pH = 9.2) gradient (2:98 to 100:0 over 25 min), affording the hydroxamic acid **19** as a white powder (0.077 g, 88%). Purity 99%. mp: 156 °C. $t_{R,LCMS} = 1.48$ min. MS (ESI-): $m/z = 207$ [M-H]⁻, MS (ESI+): $m/z = 209$ [M+H]⁺. ¹H NMR 300 MHz (DMSO-*d*₆) δ (ppm): 8.52 (t, $J = 5.5$ Hz, 1H), 7.85-7.81 (m, 2H), 7.54-7.41 (m, 3H), 3.44 (td, $J = 7.1$ Hz, $J = 5.5$ Hz, 2H), 2.26 (t, $J = 7.1$ Hz, 2H). ¹³C NMR 75 MHz (DMSO-*d*₆) δ (ppm): 167.2, 166.1, 134.4, 131.1, 128.2, 127.1, 36.0, 32.4. HRMS m/z calculated for C₁₀H₁₃N₂O₃ [M+H]⁺: 209.0926. Found: 209.0926.

N-Benzyl-3-(hydroxyamino)-3-oxo-propanamide (**20**). A solution of Meldrum's acid (0.445 g, 3.08 mmol, 1 equiv) and benzylamine (0.800 mL; 7.33 mmol, 2.37 equiv) in MeCN (2.50 mL, 1.2 M) was stirred at room temperature for 3 h. A light yellow color appeared and white crystals quickly formed. They were filtered and washed with diethyl-ether affording the carboxylic acid **20b** as white crystals (0.374 g, 63%). mp: 176 °C. $t_{R,LCMS} = 1.68$ min. MS (ESI-): $m/z = 192$ [M-H]⁻, MS (ESI+): $m/z = 194$ [M+H]⁺. To a solution of **20b** (0.340 g, 1.76 mmol, 1 equiv) in MeOH (5.90 mL, 0.3 M) at 0 °C was added dropwise thionyl chloride (0.383 μ L, 5.28 mmol,

3 equiv). The reaction mixture was stirred at room temperature for 30 min, then solvents were evaporated *in vacuo*. White crystals were obtained. These crystals were dissolved in EtOAc and washed with aqueous 5% NaHCO₃. EtOAc was evaporated *in vacuo* and methyl ester **20a** was crystallized from methanol affording colorless crystals (0.168 g, 46%). mp: 108 °C. $t_{R,LCMS}$ = 1.98 min. MS (ESI-): m/z = 206 [M-H]⁻, MS (ESI+): m/z = 208 [M+H]⁺. To a solution of **20a** (0.159 g, 0.76 mmol, 1 equiv) in MeOH (1.60 mL, 0.45 M) was added a solution of aqueous hydroxylamine 50% (1.60 mL) and KCN (0.005 g, 0.06 mmol, 0.1 equiv). The mixture was stirred 17 h at room temperature. It was concentrated under vacuum and an aqueous workup was performed using H₂O/EtOAc (1:50 (v:v)). Solvents in the organic layer were evaporated under vacuum and purified by preparative HPLC using a linear acetonitrile/water gradient, containing ammonium-acetate/formic acid buffer (pH = 9.2), starting with H₂O 98% to reach acetonitrile 100% in 25min. Pure hydroxamic acid **20** was obtained as white crystals (0.069 g, 42%). Purity 98%. mp: 135 °C. $t_{R,LCMS}$ = 1.55 min. MS (ESI-): m/z = 207 [M-H]⁻, MS (ESI+): m/z = 209 [M+H]⁺. ¹H NMR 300 MHz (DMSO-*d*₆) δ (ppm): 10.84 (s, 1H), 8.91 (s, 1H), 8.46 (t, J = 5.8 Hz, 1H), 7.34-7.20 (m, 5H), 4.28 (d, J = 5.8 Hz, 2H), 2.96 (s, 2H). ¹³C NMR 75 MHz (DMSO-*d*₆) δ (ppm): 166.3, 163.7, 139.1, 128.2, 127.2, 126.7, 42.2, 40.8. HRMS m/z calculated for C₁₀H₁₃N₂O₃ [M+H]⁺: 209.0926. Found: 209.0935.

N-Hydroxy-*N'*-phenyl succinamide (**21**). Obtained following the general procedure **B** from 3-(phenylcarbamoyl)propanoic acid. White powder (0.040 g, 12%). Purity 99%. mp: 122 °C. $t_{R,LCMS}$ = 2.20 min. MS (ESI+): m/z = 209 [M+H]⁺. ¹H NMR 300 MHz (acetone-*d*₆) δ (ppm): 7.63 (d, J = 6.9 Hz, 2H), 7.26 (t, J = 6.9 Hz, 2H), 7.02 (t, J = 6.9 Hz, 1H), 2.65 (br s, 2H), 2.46 (br s, 2H). ¹³C NMR 75 MHz (acetone-*d*₆) δ (ppm): 170.0, 169.4, 139.4, 128.6, 123.1, 119.0, 31.8, 27.5. HRMS m/z calculated for C₁₀H₁₃N₂O₃ [M+H]⁺: 209.0926. Found: 209.0923.

N-hydroxy-2-methyl-4-phenyl-butyramide (**22**). Obtained following the general procedure **B** from **22b**. White powder (0.160 g, 25%). Purity 99%. mp: 134 °C. $t_{R,LCMS} = 2.57$ min. MS (ESI+): $m/z = 194$ [M+H]⁺. ¹H NMR 300 MHz (DMSO-*d*₆) δ (ppm): 10.42 (br s, 1H), 8.72 (br s, 1H), 7.29-7.14 (m, 5H), 2.49-2.45 (m, 2H), 2.13-2.10 (m, 1H), 1.80-1.74 (m, 1H), 1.56-1.54 (m, 1H), 1.02 (d, $J = 6.6$ Hz, 3H). ¹³C NMR 75 MHz (DMSO-*d*₆) δ (ppm): 172.7, 142.3, 128.8, 128.6, 126.2, 36.9, 35.8, 33.5, 18.4. HRMS m/z calculated for C₁₁H₁₆NO₂ [M+H]⁺: 194.1181. Found: 194.1182.

2-Benzyl-4-phenyl-butanehydroxamic acid (**23**). Obtained following the general procedure **B** from **23b**. White amorphous solid (0.037 g, 13%). Purity: 95%. mp: 131 °C. $t_{R,LCMS} = 2.58$ min. MS (ESI+): $m/z = 270$ [M+H]⁺. ¹H NMR 300 MHz (DMSO-*d*₆) δ (ppm): 10.45 (br s, 1H), 8.78 (br s, 1H), 7.28-7.11 (m, 10H), 2.84 (dd, $J = 8.4$ Hz, $J = 13.5$ Hz, 1H), 2.63 (dd, $J = 6.9$ Hz, $J = 13.5$ Hz, 1H), 2.50-2.31 (m, 3H), 1.83-1.73 (m, 1H), 1.64-1.53 (m, 1H). ¹³C NMR 75 MHz (DMSO-*d*₆) δ (ppm): 171.1, 142.2, 140.2, 129.3, 128.8, 128.6, 128.5, 126.5, 126.2, 44.8, 38.6, 34.4, 33.5. HRMS m/z calculated for C₁₇H₂₀NO₂ [M+H]⁺: 270.1494. Found: 270.1503.

2-Benzenesulfonyl-*N*-hydroxy-4-phenyl-butyramide (**24**). Obtained following the general procedure **B** from **24b**. White powder (0.07 g, 63%). Purity 99%. mp: 176 °C. $t_{R,LCMS} = 2.70$ min. MS (ESI+): $m/z = 320$ [M+H]⁺. ¹H NMR 300 MHz (DMSO-*d*₆) δ (ppm): 10.94 (br s, 1H), 9.32 (br s, 1H), 7.79-7.73 (m, 3H), 7.65-7.60 (m, 2H), 7.25-7.18 (m, 3H), 7.09-7.06 (m, 2H), 3.76 (s, 1H), 2.50-2.37 (m, 2H), 1.99 (br s, 2H). ¹³C NMR 75 MHz (DMSO-*d*₆) δ (ppm): 160.7, 140.4, 137.4, 134.7, 129.6, 128.9, 128.6, 126.7, 67.1, 32.2, 28.7. HRMS m/z calculated for C₁₆H₁₈NO₄S [M+H]⁺: 320.0957. Found: 320.0956.

2-Benzenesulfonyl-*N*-hydroxy-2-methyl-4-phenyl-butyramide (**25**). Obtained following the general procedure **B** from **25a**. White powder (0.020 g, 12%). Purity 99%. mp: 159 °C. $t_{R,LCMS} = 2.82$ min. MS (ESI+): $m/z = 334$ [M+H]⁺. ¹H NMR 300 MHz (CDCl₃) δ (ppm): 7.82 (d, $J = 7.5$ Hz, 2H), 7.73-7.68 (m, 1H), 7.60-7.55 (m, 2H), 7.32-7.14 (m, 5H), 2.69-2.55 (m, 3H), 2.24-

2.14 (m, 1H), 1.58 (s, 3H). ^{13}C NMR 75 MHz (CDCl_3) δ (ppm): 165.1, 140.0, 134.7, 134.5, 130.1, 129.3, 128.6, 128.3, 126.5, 71.0, 35.1, 30.3, 16.7. HRMS m/z calculated for $\text{C}_{17}\text{H}_{20}\text{NO}_4\text{S}$ $[\text{M}+\text{H}]^+$: 334.1113. Found: 334.1113.

2-Benzyl-N-hydroxy-2-methanesulfonyl-4-phenyl-butyramide (**26**). Obtained following the general procedure **B** from **26a**. White solid (0.047g, 10%). Purity 99%. mp: 105 °C. $t_{\text{R,LCMS}}$ = 2.90 min. MS (ESI+): m/z = 348 $[\text{M}+\text{H}]^+$. ^1H NMR 300 MHz ($\text{CD}_3\text{OD}-d_4$) δ (ppm): 7.40-7.32 (m, 5H), 7.30-7.13 (m, 3H), 7.10 (d, J = 6.9 Hz, 2H), 3.85 (d, J = 13.8 Hz, 1H), 3.40 (d, J = 13.8 Hz, 1H), 3.06 (s, 3H), 2.85-2.80 (m, 2H), 2.36-2.26 (m, 1H), 2.11-2.00 (m, 1H). ^{13}C NMR 75 MHz ($\text{CD}_3\text{OD}-d_4$) δ (ppm): 165.4, 141.4, 134.7, 130.2, 128.7, 128.2, 127.9, 127.1, 125.7, 73.9, 38.2, 36.6, 35.7, 29.9. HRMS m/z calculated for $\text{C}_{18}\text{H}_{22}\text{NO}_4\text{S}$ $[\text{M}+\text{H}]^+$: 348.1270. Found: 348.1288.

(S)-2-Benzylamino-N-hydroxy-propionamide (**27**). Obtained following the general procedure **B** from **27b**. White powder (0.030 g, 8%). Purity 87%. mp: 154 °C. $t_{\text{R,LCMS}}$ = 1.22 min. MS (ESI+): m/z = 195 $[\text{M}+\text{H}]^+$. ^1H NMR 300 MHz ($\text{DMSO}-d_6$) δ (ppm): 8.81 (br s, 1H), 7.31-7.20 (m, 5H), 3.66 (d, J = 13.2 Hz, 1H), 3.49 (d, J = 13.2 Hz, 1H), 2.99 (q, J = 6.9 Hz, 1H), 1.11 (d, J = 6.9 Hz, 3H). ^{13}C NMR 75 MHz ($\text{DMSO}-d_6$) δ (ppm): 171.7, 140.9, 128.6, 128.3, 127.1, 54.4, 51.1, 19.9. HRMS m/z calculated for $\text{C}_{10}\text{H}_{15}\text{N}_2\text{O}_4$ $[\text{M}+\text{H}]^+$: 195.1134. Found: 195.1124.

(S)-2-Benzylamino-N-hydroxy-3-phenyl-propionamide (**28**). Obtained following the general procedure **B** from **28b**. White solid (0.095 g, 13%). Purity: 99%. mp: 163 °C. $t_{\text{R,LCMS}}$ = 2.25 min. MS (ESI+): m/z = 271 $[\text{M}+\text{H}]^+$. ^1H NMR 300 MHz ($\text{DMSO}-d_6$) δ (ppm): 11.00 (br s, 1H), 9.56 (br s, 1H), 9.34 (br s, 1H), 7.46-7.42 (m, 5H), 7.32-7.27 (m, 3H), 7.17 (d, J = 6.9 Hz, 2H), 4.03 (s, 2H), 3.77-3.72 (m, 2H), 3.20-3.00 (m, 2H). ^{13}C NMR 75 MHz ($\text{DMSO}-d_6$) δ (ppm): 163.3, 135.2, 132.0, 130.5, 129.8, 129.5, 129.2, 129.0, 127.7, 59.0, 49.4, 36.0. HRMS m/z calculated for $\text{C}_{16}\text{H}_{19}\text{N}_2\text{O}_2$ $[\text{M}+\text{H}]^+$: 271.1447. Found: 271.1438.

N-[(1*S*)-2-(Hydroxyamino)-1-(hydroxymethyl)-2-oxo-ethyl]-4-phenyl-benzamide (29).

Obtained following the general procedure **B** from **29b**. White solid (0.046 g, 8%). Purity 90%. mp: 179 °C. $t_{R,LCMS} = 2.53$ min. MS (ESI+): $m/z = 301$ [M+H]⁺. ¹H NMR 300 MHz (CD₃OD-*d*₄) δ (ppm): 7.97 (d, *J* = 8.1 Hz, 2H), 7.73 (d, *J* = 8.1 Hz, 2H), 7.67 (d, *J* = 7.5 Hz, 2H) 7.46 (t, *J* = 7.5 Hz, 2H), 7.38 (d, *J* = 7.5 Hz, 1H), 4.63 (t, *J* = 5.7 Hz, 2H), 3.89 (d, *J* = 5.7 Hz, 1H). ¹³C NMR 75 MHz (CD₃OD-*d*₄) δ (ppm): 168.4, 168.2, 144.6, 139.8, 132.3, 128.6, 127.8, 126.7, 126.6, 61.5, 53.9. HRMS m/z calculated for C₁₆H₁₇N₂O₄S [M+H]⁺: 301.1188. Found: 301.1198.

N-Benzyl-3-(hydroxyamino)-2-methyl-3-oxo-propanamide (30). Obtained following the general procedure **C** from commercial 1,3-diethyl 2-methylpropanedioate. White powder (0.025 g, 4%). Purity 99%. mp: 138 °C. $t_{R,LCMS} = 1.65$ min. MS (ESI-): $m/z = 221$ [M-H]⁻, MS (ESI+): $m/z = 223$ [M+H]⁺. ¹H NMR 300 MHz (DMSO-*d*₆) δ (ppm): 10.38 (br s, 1H), 8.90 (s, 1H), 8.17 (t, *J* = 5.7 Hz, 1H), 7.33-7.22 (m, 5H), 4.26 (d, *J* = 5.7 Hz, 2H), 3.07 (q, *J* = 7.1 Hz, 1H), 1.22 (d, *J* = 7.1 Hz, 3H). ¹³C NMR 75 MHz (DMSO-*d*₆) δ (ppm): 169.6, 167.4, 139.3, 128.2, 127.1, 126.7, 44.3, 42.2, 14.6. HRMS m/z calculated for C₁₁H₁₅N₂O₃ [M+H]⁺: 223.1083. Found: 223.1086.

N,2-Dibenzyl-3-(hydroxyamino)-3-oxo-propanamide (31). Obtained following the general procedure **C** from commercial 1,3-diethyl 2-benzylpropanedioate. White crystals (0.201 g, 27%). Purity 99%. TLC dichloromethane/methanol 95:05 (v:v) *R_f* = 0.55. mp: 179 °C. $t_{R,LCMS} = 2.22$ min. MS (ESI-): $m/z = 297$ [M-H]⁻, MS (ESI+): $m/z = 299$ [M+H]⁺. ¹H NMR 300 MHz (DMSO-*d*₆) δ (ppm): 10.43 (s, 1H), 8.92 (s, 1H), 8.19 (t, *J* = 5.7 Hz, 1H), 7.28-7.09 (m, 10H), 4.29 (dd, *J* = 6.1 Hz, *J* = 15.2 Hz, 1H), 4.18 (dd, *J* = 5.5 Hz, *J* = 15.2 Hz, 1H), 3.30 (t, *J* = 7.5 Hz, 1H), 3.04 (t, *J* = 5.7 Hz, 2H). ¹³C NMR 75 MHz (DMSO-*d*₆) δ (ppm): 168.1, 165.7, 139.1, 138.9, 128.8, 128.1, 127.0, 126.6, 126.1, 52.3, 42.2, 34.6. HRMS m/z calculated for C₁₇H₁₉N₂O₃ [M+H]⁺: 299.1396. Found: 299.1399.

N-Benzyl-3-(hydroxyamino)-3-oxo-2-(4-pyridylmethyl)propanamide (**32**). To a solution of commercial dimethyl malonate (1.068 g, 8.08 mmol, 1 equiv) in THF (15 mL, 0.5 M) at 0 °C was carefully added NaH 60% dispersion in mineral oil (0.679 g, 17 mmol, 2.1 equiv) the mixture was allowed to come back to room temperature and stirred for 30 min before 4-(chloromethyl)pyridine hydrochloride (1.193 g, 7.27 mmol, 0.9 equiv) was added and the mixture was stirred at 40 °C for 5 h. Solvents were evaporated *in vacuo* and the residue was purified by flash silica gel column chromatography (cyclohexane/EtOAc, 100:0 to 50:50) affording **61** as a colorless oil. $t_{R,LCMS} = 1.62$ min. MS (ESI+): $m/z = 224$ [M+H]⁺. Degradation occurs very quickly, the oil turning rapidly reddish, then blackish and solids then start to form. A degradation rate of 55% was calculated based on UV-LCMS. This intermediate (0.870 g, 23%) was engaged in the next step, following general procedure C without further purification. **32** was thus obtained as a white solid (0.02 g, 7%). Purity 99%. mp: 87 °C. $t_{R,LCMS} = 1.52$ min. MS (ESI-): $m/z = 298$ [M-H]⁻, MS (ESI+): $m/z = 300$ [M+H]⁺. ¹H NMR 300 MHz (DMSO-*d*₆) δ (ppm): 10.46 (s, 1H), 8.97 (s, 1H), 8.44 (d, $J = 1.4$ Hz, 2H), 8.26 (t, $J = 5.8$ Hz, 1H), 7.30-7.11 (m, 7H), 4.29 (dd, $J = 15.1$ Hz, $J = 6.0$ Hz, 1H), 4.19 (dd, $J = 15.1$ Hz, $J = 5.7$ Hz, 1H), 3.35 (t, $J = 7.6$ Hz, 1H), 3.06 (dd, $J = 7.6$ Hz, $J = 2.6$ Hz, 1H), 3.08 (dd, $J = 7.6$ Hz, $J = 3.5$ Hz, 1H). ¹³C NMR 75 MHz (DMSO-*d*₆) δ (ppm): 167.7, 165.3, 149.3, 147.8, 139.0, 128.2, 127.0, 126.7, 124.2, 51.0, 42.2, 33.6. HRMS m/z calculated for C₁₆H₁₈N₃O₃ [M+H]⁺: 300.1348. Found: 300.1376.

N-Benzyl-3-(hydroxyamino)-2-(2-naphthylmethyl)-3-oxo-propanamide (**33**). Meldrum's acid (0.500 g, 3.47 mmol, 1 equiv) and 2-naphthaldehyde (0.542 g, 3.47 mmol, 1 equiv) were dissolved in acetonitrile (4 mL, 1 M) and stirred at room temperature for 1 h 30 min. A solution of Hantzsch's ester (0.879 g, 3.47 mmol, 1 equiv) in methanol (3 mL) was added to the mixture, followed by L-proline (0.080 g, 0.69 mmol, 0.2 equiv). The resulting mixture was stirred overnight at room temperature. A precipitate was formed and dissolved when the mixture was

diluted with acetonitrile. Solvents were evaporated *in vacuo* and the residue was triturated in methanol, affording 2,2-dimethyl-5-(2-naphthylmethyl)-1,3-dioxane-4,6-dione **60** as a white solid (0.676 g, 68%). Purity 99%. $t_{R,LCMS} = 1.17$ min. MS (ESI+): $m/z = 285$ [M+H]⁺. ¹H NMR 300 MHz (CDCl₃) δ (ppm): 7.82-7.76 (m, 4H), 7.50-7.42 (m, 3H), 3.84 (t, $J = 4.9$ Hz, 1H), 3.65 (d, $J = 4.9$ Hz, 2H), 1.73 (s, 3H), 1.50 (s, 3H). ¹³C NMR 75 MHz (CDCl₃) δ (ppm): 165.4, 134.9, 133.5, 132.6, 128.7, 128.4, 128.0, 127.9, 127.7, 126.3, 126.0, 105.3, 48.4, 32.3, 28.6, 27.3. A solution of **60** (0.097 g, 0.34 mmol, 1 equiv) and benzylamine (0.037 mL, 0.34 mmol, 1 equiv) in acetonitrile (0.480 mL, 0.7 M) was heated under microwaves irradiation at 80 °C for 1 h 45 min. The product spontaneously crystallized from the light yellow reaction mixture at room temperature. It was filtered off and washed with diethyl ether, affording 3-(benzylamino)-2-(2-naphthylmethyl)-3-oxo-propanoic acid **33b** (0.112 g, 95%) as light-yellow crystals. $t_{R,LCMS} = 2.62$ min. MS (ESI-): $m/z = 332$ [M-H]⁻, MS (ESI+): $m/z = 334$ [M+H]⁺. To a solution of carboxylic acid **33b** (0.112 g, 0.33 mmol, 1 equiv) in methanol (1 mL, 0.3 M) at 0 °C was added dropwise thionyl chloride (0.073 mL, 1.00 mmol, 3 equiv). The reaction mixture was stirred at room temperature for 5 h before methanol was evaporated *in vacuo*. A white powder was obtained and dissolved in ethyl acetate, washed with sat. aqueous NaHCO₃ twice. Organic fractions were pooled and evaporated under vacuum, affording methyl 3-(benzylamino)-2-(2-naphthylmethyl)-3-oxo-propanoate **33a** as a white powder (0.105 g, 89%). $t_{R,LCMS} = 2.98$ min. MS (ESI-): $m/z = 346$ [M-H]⁻, MS (ESI+): $m/z = 348$ [M+H]⁺. To a solution of **33a** (0.105 g, 0.30 mmol, 1 equiv) in MeOH (0.660 mL, 0.45 M) was added a solution of aqueous hydroxylamine 50% (0.660 mL) and KCN (0.02 g, 0.028 mmol, 0.1 equiv). The mixture was stirred for 4 h at room temperature. It was concentrated under vacuum and an aqueous workup was performed using H₂O/EtOAc (1:50 (v:v)). Solvents in the organic layer were evaporated under vacuum and the residue was purified by preparative HPLC using a linear acetonitrile/water gradient, containing ammonium-acetate/formic acid buffer (pH = 9.2),

starting with H₂O 98% to reach acetonitrile 100% in 25min. Pure hydroxamic acid **33** was obtained as a white powder (0.039 g, 36%). Purity 99%. $t_{R,LCMS} = 2.52$ min. MS (ESI-): $m/z = 347$ [M-H]⁻, MS (ESI+): $m/z = 349$ [M+H]⁺. ¹H NMR 300 MHz (DMSO-*d*₆) δ (ppm): 10.43 (s, 1H), 8.93 (s, 1H), 8.25 (t, $J = 5.9$ Hz, 1H), 7.88-7.78 (m, 3H), 7.69 (s, 1H), 7.51-7.36 (m, 3H), 7.15-7.01 (m, 5H), 4.31 (dd, $J = 6.2$ Hz, $J = 15.3$ Hz, 1H), 4.17 (dd, $J = 5.4$ Hz, $J = 15.3$ Hz, 1H), 3.43 (t, $J = 7.5$ Hz, 1H), 3.22 (t, $J = 7.5$ Hz, 2H). ¹³C NMR 75 MHz (DMSO-*d*₆) δ (ppm): 168.1, 165.7, 139.0, 136.6, 133.0, 131.8, 128.0, 127.7, 127.6, 127.5, 127.4, 127.0, 126.9, 125.9, 125.4, 52.3, 42.2, 34.9. HRMS m/z calculated for C₂₁H₂₁N₂O₃ [M+H]⁺: 349.1552. Found: 349.1545.

N,2-Dibenzyl-3-(hydroxyamino)-2-methyl-3-oxo-propanamide (**34**). To a solution of alcoholate ethoxysodium (3.8 mL, 13.33 mmol, 1.2 equiv) cooled to 0 °C with an ice bath was added commercial diethyl 2-methylpropanedioate (1 mL, 8.61 mmol, 1 equiv). Then the mixture was heated to 50 °C for 1 h and bromomethylbenzene (0.927 mL, 7.75 mmol, 0.9 equiv) was added. The mixture was heated again to 50 °C during 19 h and solvent was evaporated under vacuum. The crude product was dissolved in EtOAc and aqueous sat. NaHCO₃ then the organic layer was washed three time with aqueous sat. NaHCO₃ and one time with aqueous NaOH 10% then dried with MgSO₄ and evaporated under vacuum to give not pure diethyl 2-benzyl-2-methylpropanedioate **62** (1.409 g, 37%) as an orange oil. Purity 60%. $t_{R,LCMS} = 3.28$ min. MS (ESI+): $m/z = 265$ [M+H]⁺. This synthesis intermediate was used for general procedure C without further purification. **34** was obtained as a white solid (0.089 g, 12%). Purity 99%. mp: 66 °C. $t_{R,LCMS} = 2.33$ min. MS (ESI-): $m/z = 311$ [M-H]⁻, MS (ESI+): $m/z = 313$ [M+H]⁺. ¹H NMR 300 MHz (DMSO-*d*₆) δ (ppm): 8.23 (t, $J = 5.5$ Hz, 1H), 7.32-7.08 (m, 10H), 4.28 (t, $J = 5.5$ Hz, 2H), 3.17 (d, $J = 13.2$ Hz, 1H), 3.08 (d, $J = 13.2$ Hz, 1H), 1.16 (s, 1H). ¹³C NMR 75 MHz (DMSO-*d*₆) δ (ppm): 171.4, 169.1, 139.4, 137.1, 130.1, 128.1, 127.8, 127.1, 126.6, 126.3, 52.9, 42.5, 41.7, 18.8. HRMS m/z calculated for C₁₈H₂₁N₂O₃ [M+H]⁺: 313.1552. Found: 313.1560.

N-Benzyl-3-(hydroxyamino)-2,2-dimethyl-3-oxo-propanamide (**35**). Obtained following the general procedure **C** from commercial 1,3-diethyl 2,2-dimethylpropanedioate. White solid (0.02 g, 7%). Purity 99%. mp: 133 °C. $t_{R,LCMS} = 1.73$ min. MS (ESI-): $m/z = 235$ [M-H]⁻, MS (ESI+): $m/z = 237$ [M+H]⁺. ¹H NMR 300 MHz (DMSO-*d*₆) δ (ppm): 8.33 (s, 1H), 8.07 (t, *J* = 5.8 Hz, 1H), 7.36-7.18 (m, 5H), 4.26 (d, *J* = 5.8 Hz, 2H), 1.31 (s, 6H). ¹³C NMR 75 MHz (DMSO-*d*₆) δ (ppm): 172.5, 170.1, 139.6, 128.1, 126.8, 126.5, 52.3, 48.2, 23.2. HRMS m/z calculated for C₁₂H₁₇N₂O₃ [M+H]⁺: 237.1239. Found: 237.1247.

N-Benzyl-1-(hydroxycarbamoyl)cyclopropanecarboxamide (**36**). Obtained following the general procedure **C** from commercial 1,1-diethyl cyclopropane-1,1-dicarboxylate. Colorless oil (0.02 g, 4%). Purity 99%. $t_{R,LCMS} = 1.73$ min. MS (ESI-): $m/z = 233$ [M-H]⁻, MS (ESI+): $m/z = 235$ [M+H]⁺. ¹H NMR 300 MHz (CD₃OD-*d*₄) δ (ppm): 8.54 (s, 1H), 7.34-7.21 (m, 5H), 4.40 (s, 2H), 1.40-1.28 (ddd, *J* = 5.9 Hz, *J* = 8.7 Hz, *J* = 19.4 Hz, 4H). ¹³C NMR 75 MHz (CD₃OD-*d*₄) δ (ppm): 172.0, 170.0, 139.8, 129.4, 128.4, 128.2, 44.4, 28.4, 15.5. HRMS m/z calculated for C₁₂H₁₅N₂O₃ [M+H]⁺: 235.1083. Found: 235.1092.

2-Benzyl-*N*-[(4-fluorophenyl)methyl]-3-(hydroxyamino)-3-oxo-propanamide (**39**). Obtained following the general procedure **C** from commercial 1,3-diethyl 2-benzylpropanedioate. Light yellow crystals (0.046 g, 4%). Purity 97%. mp: 185 °C. $t_{R,LCMS} = 2.63$ min. MS (ESI-): $m/z = 315$ [M-H]⁻, MS (ESI+): $m/z = 317$ [M+H]⁺. ¹H NMR 300 MHz (CD₃OD-*d*₄) δ (ppm): 7.25-7.19 (m, 5H), 7.13-7.09 (m, 2H), 7.00-6.94 (m, 2H), 4.36 (d, *J* = 15.0 Hz, 1H), 4.23 (d, *J* = 15.0 Hz, 1H), 3.33 (t, *J* = 7.8 Hz, 1H), 3.15 (d, *J* = 7.8 Hz, 2H). ¹³C NMR 75 MHz (CD₃OD-*d*₄) δ (ppm): 168.7, 165.0, 161.7 (d, *J*_{CF} = 22.4 Hz), 139.3, 135.6 (d, *J*_{CF} = 2.3 Hz), 130.3 (d, *J*_{CF} = 8.4 Hz), 130.0, 129.5, 127.7, 116.2 (d, *J*_{CF} = 22.4 Hz), 54.7, 43.4, 37.2. HRMS m/z calculated for C₁₇H₁₈FN₂O₃ [M+H]⁺: 317.1301. Found: 317.1303.

2-Benzyl-3-(hydroxyamino)-3-oxo-N-(4-pyridylmethyl)propanamide (43). Obtained following the general procedure **C** from commercial 1,3-diethyl 2-benzylpropanedioate. White powder (0.080 g, 22%). Purity 98%. mp: 204 °C. $t_{R,LCMS} = 1.37$ min. MS (ESI-): $m/z = 298$ [M-H]⁻, MS (ESI+): $m/z = 300$ [M+H]⁺. ¹H NMR 300 MHz (CD₃OD-*d*₄) δ (ppm): 8.37 (dd, $J = 1.5$ Hz, $J = 4.5$ Hz, 2H), 7.28-7.23 (m, 5H), 7.11 (dd, $J = 1.5$ Hz, $J = 4.5$ Hz, 2H), 4.46 (d, $J = 16.5$ Hz, 1H), 4.31 (d, $J = 16.5$ Hz, 1H), 3.40 (t, $J = 7.8$ Hz, 1H), 3.19 (d, $J = 7.8$ Hz, 2H). ¹³C NMR 75 MHz (CD₃OD-*d*₄) δ (ppm): 171.3, 168.6, 150.5, 149.9, 139.3, 130.1, 129.6, 127.8, 123.6, 54.7, 42.9, 36.9. HRMS m/z calculated for C₁₆H₁₈N₃O₃ [M+H]⁺: 300.1348. Found: 300.1361.

1-Benzoylpyrrolidine-3-carbohydroxamic acid (44). To a solution of commercial O-1-tert-butyl O-3-methyl pyrrolidine-1,3-dicarboxylate (0.200 g, 0.87 mmol, 1 equiv) in anhydrous DCM (2 mL, 0.43 M) was added dropwise TFA (0.513 mL, 6.97 mmol, 8 equiv) at 0 °C. The cooling bath was removed and the mixture was stirred 1 h at room temperature. Then DCM was evaporated in vacuo, the residue was dissolved in DCM and evaporated again under vacuum (5 cycles) to eliminate TFA. Methyl pyrrolidine-3-carboxylate **70** (0.112 g, 99%) was obtained as yellow oil. To a solution of amine **70** (0.112 g, 0.86 mmol, 1 equiv) and DIPEA (0.161 mL, 0.95 mmol, 1.1 equiv), in anhydrous DCM (2 mL, 0.43 M) at 0 °C was added dropwise benzoyl chloride (0.101 mL, 0.87 mmol, 1 equiv). The ice bath was removed and the solution was stirred 2 h to rt. Solvent was evaporated under vacuum and the residue was partitioned between aqueous HCl (1M) and EtOAc. The aqueous phase was extracted two times with EtOAc and the three organic layers were pooled, dried over MgSO₄ and evaporated to give a yellow crude product which was purified by flash column chromatography cyclohexane/EtOAc. Pure methyl 1-benzoylpyrrolidine-3-carboxylate **44a** (0.167 g, 62%) was obtained as colorless oil. $t_{R,LCMS} = 2.45$ min. MS (ESI+): $m/z = 234$ [M+H]⁺. To a solution of **44a** (0.167 g, 0.71 mmol, 1 equiv) in MeOH (2.97 mL, 0.24 M) was added a solution of aqueous hydroxylamine 50% (2.97 mL, aq. NH₂OH/MeOH 1:1 (v:v)) and KCN (0.023 g, 0.35 mmol, 0.5 equiv). The solution was

stirred overnight at room temperature (convenience). Crude product was concentrated under vacuum and an aqueous workup was performed using H₂O/EtOAc (1:50 (v:v)) then the aqueous layer was dissolved in a mixture of aqueous 15% KOH/NaClO 75:25 (v:v) and discarded in an appropriate waste tank. The organic layer was evaporated under vacuum and purified by preparative HPLC using a linear acetonitrile/water gradient, containing ammonium-acetate/formic acid buffer (pH = 3.8), starting with H₂O 98% to reach acetonitrile 100% in 25min. Pure hydroxamic acid **44** was obtained as colorless oil (0.027 g, 16%). Purity 97%. $t_{R,LCMS} = 1.37$ min. MS (ESI-): $m/z = 233$ [M-H]⁻, MS (ESI+): $m/z = 235$ [M+H]⁺. ¹H NMR 300 MHz (CD₃OD-*d*₄) δ (ppm): 8.52 (s, 1H), 7.54-7.50 (m, 2H), 7.49-7.43 (m, 3H), 3.85-3.37 (m, 2H), 3.69-3.50 (m, 2H), 2.94 (t, $J = 7.6$ Hz, 1H), 2.23-2.17 (m, 1H), 2.11 (dd, $J = 6.8$ Hz, $J = 13.8$ Hz, 1H). ¹³C NMR 75 MHz (CD₃OD-*d*₄) δ (ppm): 172.3, 171.6, 137.7, 131.4, 129.6, 128.1, 42.7, 41.1, 31.0, 29.2. HRMS m/z calculated for C₁₂H₁₅N₂O₃ [M+H]⁺: 235.1083. Found: 235.1114.

N-[3-(Hydroxyamino)-3-oxo-2-(1-piperidyl)propyl]benzamide (**45**). To a solution of commercial methyl 3-amino-2-(1-piperidyl)propanoate **74** (0.437 g, 2.34 mmol, 1.1 equiv) and DIPEA (0.396 mL, 2.32 mmol, 1.1 equiv) in anhydrous DCM at 0 °C was added benzoyl chloride (0.248 mL, 2.13 mmol, 1 equiv). The solution was allowed to warm at room temperature and stirred 1 h. Then DCM was evaporated under pressure and the residue was partitioned between aqueous HCl 1M and EtOAc. The aqueous layer washed twice by EtOAc and basified with K₂CO₃. Then the desired product was extracted by EtOAc. Solvent was evaporated in vacuo to afford methyl 3-benzamido-2-(1-piperidyl)propanoate **45a** as yellow oil (0.257 g, 41%). $t_{R,LCMS} = 1.86$ min. MS (ESI+): $m/z = 291$ [M+H]⁺. To a solution of **45a** (0.100 g, 0.35 mmol, 1 equiv) in MeOH (1.43 mL, 0.25 M) was added a solution of aqueous hydroxylamine 50% (1.43 mL, aq. NH₂OH/MeOH 1:1 (v:v)) and KCN (0.011 g, 0.17 mmol, 0.5 equiv). The mixture was stirred overnight at room temperature (convenience). Crude

product was concentrated under vacuum and an aqueous workup was performed using H₂O/EtOAc (1:50 (v:v)) then the aqueous layer was dissolved in a mixture of aqueous 15% KOH/NaClO 75:25 (v:v) and discarded in an appropriate waste tank. The organic layer was evaporated under vacuum and purified by preparative HPLC using a linear acetonitrile/water gradient, containing ammonium-acetate/formic acid buffer (pH = 9.2), starting with H₂O 98% to reach acetonitrile 100% in 25min. Pure hydroxamic acid **45** was obtained as brown solid (0.029 g, 29%). Purity 98%. mp: 93 °C. $t_{R,LCMS}$ = 1.48 min. MS (ESI-): m/z = 290 [M-H]⁻, MS (ESI+): m/z = 292 [M+H]⁺. ¹H NMR 300 MHz (CD₃OD-*d*₄) δ (ppm): 8.42 (br s, 1H), 7.88-7.78 (d, J = 7.2 Hz, 2H), 7.56-7.42 (m, 3H), 3.80 (dd, J = 6.2 Hz, J = 13.2 Hz, 1H), 3.62 (dd, J = 7.8 Hz, J = 13.2 Hz, 1H), 2.72-2.67 (q, J = 5.4 Hz, J = 9.2 Hz, 4H), 1.62 (m, 4H), 1.46-1.51 (q, J = 5.4 Hz, J = 11.1 Hz, 2H). ¹³C NMR 75 MHz (CD₃OD-*d*₄) δ (ppm): 170.4, 168.9, 135.6, 132.8, 129.6, 128.3, 66.3, 42.5, 39.5, 27.0, 25.3. HRMS m/z calculated for C₁₅H₂₂N₃O₃ [M+H]⁺: 292.1661. Found: 292.1693.

(*S*)-2-Benzenesulfonylamino-*N*-hydroxy-3-methyl-butylamide (**46**). Obtained following the general procedure **B** from **46b**. Pink solid (0.080 g, 12%). Purity 99%. mp: 160 °C. $t_{R,LCMS}$ = 1.80 min. MS (ESI+): m/z = 273 [M+H]⁺. ¹H NMR 300 MHz (DMSO-*d*₆) δ (ppm): 10.49 (br s, 1H), 8.77 (br s, 1H), 7.92 (d, J = 9.0 Hz, 1H), 7.78-7.74 (m, 2H), 7.62-7.51 (m, 3H), 3.28 (t, J = 8.4 Hz, 1H), 1.78-1.71 (m, 1H), 0.73 (d, J = 6.6 Hz, 3H), 0.70 (d, J = 6.6 Hz, 3H). ¹³C NMR 75 MHz (DMSO-*d*₆) δ (ppm): 167.1, 142.0, 132.6, 129.3, 126.8, 60.2, 31.2, 19.4, 19.0. HRMS m/z calculated for C₁₁H₁₇N₂O₄S [M+H]⁺: 273.0909. Found: 273.0898.

(*S*)-2-Benzenesulfonylamino-*N*-hydroxy-3-phenyl-propionamide (**47**). Obtained following the general procedure **B** from **47b**. White powder (0.020 g, 11%). Purity 97%. mp: 97 °C. $t_{R,LCMS}$ = 2.47 min. MS (ESI+): m/z = 321 [M+H]⁺. ¹H NMR 300 MHz (acetone-*d*₆) δ (ppm): 7.71-7.54 (m, 5H), 7.48-7.10 (m, 5H), 3.96-3.90 (m, 1H), 2.75 (dd, J = 7.5 Hz, J = 13.5 Hz, 2H). ¹³C

NMR 75 MHz (acetone- d_6) δ (ppm): 166.9, 141.2, 136.6, 132.3, 129.3, 128.9, 128.2, 126.7, 126.6, 55.9, 38.9. HRMS m/z calculated for $C_{15}H_{17}N_2O_4S$ $[M+H]^+$: 321.0909. Found: 321.0916. *(R)*-2-(Benzenesulfonyl-benzyl-amino)-*N*-hydroxy-3-methyl-butylamide (**48**). Obtained following the general procedure **B** from **48a**. Colorless oil (0.02 g, 4%). Purity 99%. $t_{R,LCMS}$ = 2.92 min. MS (ESI+): m/z = 363 $[M+H]^+$. 1H NMR 300 MHz (acetone- d_6) δ (ppm): 7.71-7.68 (m, 2H), 7.58-7.52 (m, 1H), 7.46-7.40 (m, 4H), 7.21-7.19 (m, 3H), 4.77 (s, 2H), 3.94 (d, J = 10.8 Hz, 1H), 2.05 (m, 1H), 0.79 (d, J = 6.6 Hz, 3H), 0.79 (d, J = 6.6 Hz, 3H). ^{13}C NMR 75 MHz (acetone- d_6) δ (ppm): 166.2, 141.1, 137.9, 132.3, 129.2, 128.7, 127.8, 127.1, 127.0, 63.8, 48.1, 26.6, 18.9, 18.6. HRMS m/z calculated for $C_{18}H_{23}N_2O_4S$ $[M+H]^+$: 363.1379. Found: 363.1372.

(R)-2-(Benzenesulfonyl-benzyl-amino)-3-phenyl-*N*-hydroxy-propionamide (**49**). Obtained following the general procedure **B** from **49b**. Colorless oil (0.020 g, 4%). Purity 98%. $t_{R,LCMS}$ = 3.07 min. MS (ESI+): m/z = 411 $[M+H]^+$. 1H NMR 300 MHz (acetone- d_6) δ (ppm): 7.82-7.79 (m, 2H), 7.61 (t, J = 7.5 Hz, 1H), 7.52 (t, J = 7.5 Hz, 2H), 7.39 (d, J = 6.6 Hz, 2H), 7.27-7.15 (m, 6H), 7.03-7.01 (m, 2H), 4.81 (s, 2H), 4.56 (dd, J = 4.8 Hz, J = 10.2 Hz, 1H), 3.14 (dd, J = 10.2 Hz, J = 13.2 Hz, 1H), 2.60 (dd, J = 4.8 Hz, J = 13.2 Hz, 1H). ^{13}C NMR 75 MHz (acetone- d_6) δ (ppm): 165.5, 140.5, 138.7, 136.7, 132.7, 129.2, 129.0, 128.3, 128.2, 127.9, 127.2, 126.9, 126.6, 58.8, 48.3, 37.1. HRMS m/z calculated for $C_{22}H_{23}N_2O_4S$ $[M+H]^+$: 411.1379. Found: 411.1395.

4-(Benzenesulfonamido)tetrahydropyran-4-carboxylic acid (**50**). To a solution of commercial methyl 4-aminooxane-4-carboxylate (0.105 g, 0.66 mmol, 1 equiv) in pyridine (0.942 mL, 0.7 M) was added dropwise liquid benzenesulfonyl chloride (0.101 mL, 0.79 mmol, 1.2 equiv). This solution was stirred 2 h at room temperature (starts light yellow then becomes dark red). The mixture was partitioned between EtOAc and aq. HCl 1 M and the organic phase was washed once again with aq. HCl 1 M. Celite was added to the organic phase and EtOAc

was evaporated under vacuum affording a solid deposit purified by flash column chromatography cyclohexane 100% to cyclohexane/EtOAc 1:1 (v:v). Colorless oil (0.179 g, 66%). Purity 98%. TLC cyclohexane 100% $R_f = 0.05$. TLC cyclohexane/EtOAc 1:1 (v:v) $R_f = 0.75$. $t_{R,LCMS} = 2.12$ min. MS (ESI+): $m/z = 298$ $[M+H]^+$, MS (ESI+): $m/z = 300$ $[M+H]^+$. 1H NMR 300 MHz ($CDCl_3$) δ (ppm): 7.87-7.84 (m, 2H), 7.57-7.47 (m, 3H), 3.60-3.56 (m, 4H), 3.47 (s, 3H), 2.11-2.03 (m, 2H), 1.91-1.85 (m, 2H). ^{13}C NMR 75 MHz ($CDCl_3$) δ (ppm): 172.8, 141.1, 132.9, 129.2, 127.3, 63.0, 59.1, 52.6, 33.2. To a solution of methyl ester **50a** (0.018 g, 0.06 mmol, 1 equiv) in MeOH (0.133 mL, 0.45 M) was added aqueous hydroxylamine 50% (0.133 mL, 1.98 mmol, 33 equiv) and solid KCN (0.001 g, 0.06 mmol, 0.1 equiv). The mixture was stirred 48h (convenience) at room temperature. The crude product was concentrated under vacuum and the residue was dissolved in acetonitrile with some drops of acidic water (0.1% formic acid) under the fume hood filtered and the solution was purified by preparative HPLC using a linear acetonitrile/water gradient, containing ammonium-acetate/formic acid buffer (pH = 3.8), starting with H₂O 98% to reach acetonitrile 100% in 25min. CH₃CN was evaporated under vacuum (37 °C under 148 mbar) and aqueous solution was sublimated affording **50** as a white powder (0.011 g, 57%). Purity 95%. mp: 61 °C. $t_{R,LCMS} = 1.57$ min. MS (ESI-): $m/z = 299$ $[M-H]^-$, MS (ESI+): $m/z = 301$ $[M+H]^+$. 1H NMR 300 MHz ($DMSO-d_6$) δ (ppm): 10.40 (s, 1H), 8.71 (s, 1H), 7.81-7.78 (m, 2H), 7.61-7.52 (m, 3H), 3.40-3.24 (m, 4H), 1.87-1.76 (m, 4H). ^{13}C NMR 75 MHz ($DMSO-d_6$) δ (ppm): 169.4, 143.1, 132.1, 128.9, 126.2, 62.4, 58.1, 32.8. HRMS m/z calculated for C₁₂H₁₇N₂O₅S $[M+H]^+$: 301.0858. Found: 301.0860.

2-(Benzenesulfonyl)-3,4-dihydro-1H-isoquinoline-3-carboxylic acid (51). To a solution of commercial 1,2,3,4-tetrahydroisoquinoline-3-carboxylic acid (0.200 g, 0.94 mmol, 1 equiv) in anhydrous methanol (3.12 mL, 0.3 M) under argon at 0 °C was added dropwise SOCl₂ (0.204 mL, 2.80 mmol, 3 equiv). The mixture was stirred at room temperature 10 days then the mixture was dissolved in EtOAc (10 mL) and washed with water. The aqueous phase was extracted 2

times with EtOAc. Organic phases were pooled, dried over MgSO₄ and evaporated under vacuum. Methyl ester product **79** was obtained as white powder (0.120 g, 64%). $t_{R,LCMS} = 1.53$ min. MS (ESI+): $m/z = 192$ [M+H]⁺. ¹H NMR 300 MHz (DMSO-*d*₆) δ (ppm): 7.25 (s, 4H), 4.50 (m, 1H), 4.30 (s, 2H), 3.79 (s, 3H), 3.28 (dd, $J = 3.8$ Hz, $J = 16.8$ Hz, 1H), 3.17 (m, 1H). To a solution of secondary amine **79** (0.120 g, 0.62 mmol, 1 equiv) in anhydrous DCM (2 mL, 0.3 M) at 0 °C was added liquid TEA (0.254 mL, 1.88 mmol, 3 equiv) and benzenesulfonyl chloride (0.096 mL, 0.75 mmol, 1.2 equiv) then the cooling bath was removed and the solution was stirred 3 h at rt. Solvent was evaporated under reduced pressure and the residue was dissolved in aqueous sat. NaHCO₃ and EtOAc. The product was extracted 2 times with EtOAc, dried over MgSO₄ and evaporated in vacuo. The residue was purified by flash column chromatography cyclohexane/ethyl acetate to afford the desired sulfonamide **51a** as colorless oil (0.048 g, 23%). $t_{R,LCMS} = 2.97$ min. MS (ESI+): $m/z = 332$ [M+H]⁺. To a solution of methyl ester (0.023 g, 0.07 mmol, 1 equiv) in MeOH (0.298 mL, 0.23 M) was added a solution of aqueous hydroxylamine 50% (0.298 mL, aq. NH₂OH/MeOH 1:1 (v:v)) and KCN (0.002 g, 0.03 mmol, 0.5 equiv). The solution was stirred overnight at room temperature (convenience). Crude product was concentrated under vacuum and an aqueous workup was performed using H₂O/EtOAc (1:50 (v:v)) then the aqueous layer was dissolved in a mixture of aqueous 15% KOH/NaClO 75:25 (v:v) and discarded in an appropriate waste tank. The organic layer was evaporated under vacuum and purified by preparative HPLC using a linear acetonitrile/water gradient, containing ammonium-acetate/formic acid buffer (pH = 3.8), starting with H₂O 98% to reach acetonitrile 100% in 25min. Pure hydroxamic acid **51** was obtained as white powder (0.009 g, 41%). Purity 99%. mp: 116 °C. $t_{R,LCMS} = 2.27$ min. MS (ESI-): $m/z = 331$ [M-H]⁻, MS (ESI+): $m/z = 333$ [M+H]⁺. ¹H NMR 300 MHz (CD₃OD-*d*₄) δ (ppm): 7.79 (m, 2H), 7.61 (tt, $J = 1.4$ Hz, $J = 7.5$ Hz, 1H), 7.46 (tt, $J = 1.4$ Hz, $J = 7.5$ Hz, 2H), 7.11-7.00 (m, 4H), 4.55 (d, $J = 4.7$ Hz, 2H), 4.47 (t, $J = 5.8$ Hz, 1H), 3.01 (dd, $J = 5.6$ Hz, $J = 15.5$ Hz, 1H), 2.78 (dd, $J = 6.4$

Hz, $J = 15.5$ Hz, 1H). ^{13}C NMR 75 MHz ($\text{CD}_3\text{OD}-d_4$) δ (ppm): 170.2, 139.3, 134.2, 134.1, 133.8, 130.3, 128.8, 128.6, 128.5, 127.8, 127.2, 56.1, 47.0, 32.1. HRMS m/z calculated for $\text{C}_{16}\text{H}_{17}\text{N}_2\text{O}_4\text{S}$ $[\text{M}+\text{H}]^+$: 333.0909. Found: 333.0928.

(E)-3-(2,4-Dichloro-phenyl)-*N*-hydroxy-acrylamide (**52**). Obtained following the general procedure **B** from **52b**. White powder (0.030 g, 6%). Purity 99%. mp: 175 °C. $t_{\text{R,LCMS}} = 2.63$ min. MS (ESI+): $m/z = 232$ $[\text{M}+\text{H}]^+$. ^1H NMR 300 MHz ($\text{DMSO}-d_6$) δ (ppm): 10.89 (br s, 1H), 9.16 (br s, 1H), 7.73-7.64 (m, 3H), 7.48 (d, $J = 15.9$ Hz, 1H), 6.53 (d, $J = 15.9$ Hz, 1H). ^{13}C NMR 75 MHz ($\text{DMSO}-d_6$) δ (ppm): 162.3, 134.9, 134.5, 132.9, 132.2, 129.9, 129.3, 128.5, 123.5. HRMS m/z calculated for $\text{C}_9\text{H}_8\text{NO}_2\text{Cl}_2$ $[\text{M}+\text{H}]^+$: 231.9932. Found: 231.9935.

(E)-3-Biphenyl-4-yl-*N*-hydroxy-acrylamide (**53**). Obtained following the general procedure **B** from commercial (2E)-3- $\{[1,1'$ -biphenyl]-4-yl $\}$ prop-2-enoic acid. White powder (0.110 g, 38%). Purity 99%. mp: 168 °C. $t_{\text{R,LCMS}} = 2.73$ min. MS (ESI+): $m/z = 240$ $[\text{M}+\text{H}]^+$. ^1H NMR 300 MHz ($\text{DMSO}-d_6$) δ (ppm): 10.78 (s, 1H), 9.05 (br s, 1H), 7.73-7.63 (m, 6H), 7.53-7.35 (m, 4H), 6.50 (d, $J = 14.4$ Hz, 1H). ^{13}C NMR 75 MHz ($\text{DMSO}-d_6$) δ (ppm): 163.2, 141.4, 139.8, 138.3, 134.4, 129.5, 128.6, 128.3, 127.6, 127.1, 119.6. HRMS m/z calculated for $\text{C}_{15}\text{H}_{14}\text{NO}_2$ $[\text{M}+\text{H}]^+$: 240.1025. Found: 240.1007.

(E)-*N*-Hydroxy-3-{4[(phenylamino)sulfonyl]phenyl}prop-2-enamide (**54**). Obtained following the general procedure **B** from **54b**. Pink solid (0.080 g, 18%). Purity 99%. mp: 171 °C. $t_{\text{R,LCMS}} = 2.47$ min. MS (ESI+): $m/z = 319$ $[\text{M}+\text{H}]^+$. ^1H NMR 300 MHz ($\text{DMSO}-d_6$) δ (ppm): 10.85 (br s, 1H), 10.32 (br s, 1H), 9.12 (br s, 1H), 7.76-7.68 (m, 4H), 7.43 (d, $J = 15.9$ Hz, 1H), 7.24 (t, $J = 7.5$ Hz, 2H), 7.08 (d, $J = 7.5$ Hz, 1H), 7.00 (t, $J = 7.5$ Hz, 2H), 6.52 (d, $J = 15.9$ Hz, 1H). ^{13}C NMR 75 MHz ($\text{DMSO}-d_6$) δ (ppm): 162.5, 140.1, 139.5, 138.0, 136.9, 129.6, 128.5, 127.7, 124.7, 122.8, 120.6. HRMS m/z calculated for $\text{C}_{15}\text{H}_{15}\text{N}_2\text{O}_4\text{S}$ $[\text{M}+\text{H}]^+$: 319.0753. Found: 319.0764.

(E)-3-[2-Butyl-1-(2-diethylamino-ethyl)-1*H*-benzimidazol-5-yl]-*N*-hydroxy-acrylamide (**55**).

Obtained following the general procedure **B** from **55b**. Yellow oil (0.22 g, 57%). Purity 97%.

$t_{R,LCMS} = 2.19$ min. MS (ESI+): $m/z = 357$ [M+H]⁺. ¹H NMR 300 MHz (DMSO-*d*₆) δ (ppm): 9.50 (br s, 2H), 7.76 (s, 1H), 7.60 (d, $J = 15.9$ Hz, 1H), 7.47-7.44 (m, 2H), 6.45 (d, $J = 15.9$ Hz, 1H), 3.35-3.30 (m, 10H), 3.12-3.05 (m, 4H), 2.89 (t, $J = 7.8$ Hz, 2H), 1.82 (m, 2H), 1.48 (m, 2H), 1.18 (t, $J = 7.8$ Hz, 3H). ¹³C NMR 75 MHz (DMSO-*d*₆) δ (ppm): 163.7, 156.8, 143.1, 139.9, 136.7, 136.3, 129.3, 121.7, 119.6, 115.7, 110.7, 47.0, 46.1, 40.2, 29.2, 26.4, 22.4, 14.2, 9.0. HRMS m/z calculated for C₂₀H₃₁N₄O₂ [M+H]⁺: 359.2447. Found: 359.2447.

N-Hydroxy-3,3-diphenyl-acrylamide (**56**). Obtained following the general procedure **B** from **56b**. White solid (0.44 g, 46%). Purity: 99%. mp: 134 °C. $t_{R,LCMS} = 2.63$ min. MS (ESI+): $m/z = 240$ [M+H]⁺. ¹H NMR 300 MHz (DMSO-*d*₆) δ (ppm): 10.60 (br s, 1H), 8.80 (br s, 1H), 7.34-7.13 (m, 11H), 6.27 (s, 1H). ¹³C NMR 75 MHz (DMSO-*d*₆) δ (ppm): 163.2, 150.1, 141.9, 139.3, 129.1, 128.9, 128.1, 128.1. HRMS m/z calculated for C₁₅H₁₄NO₂ [M+H]⁺: 240.1025. Found: 240.1029.

General Biology

Ethylenediaminetetraacetic acid (EDTA), 5,5'-dithiobis(2-nitrobenzoic acid) (DTNB), phenylmethanesulfonyl fluoride (PMSF), bis-(4-nitrophenyl)-phosphate (BNPP), ethopropazine hydrochloride (profenamine), enalapril maleate salt, eucatropine hydrochloride and prasugrel were obtained from Sigma-Aldrich, tacrine hydrochloride from Tocris. Huprine 2 was obtained as previously described.³⁵ Trandolapril was obtained from Sequoia Research Products. Solvents were from common sources and of LC-MS grade. Stock solutions of all compounds were prepared in methanol at a concentration of 1 mM. Rat plasma, and human plasma, mixed gender, were purchased from Seralab. Rat whole blood male and female were purchased from Charles River, France (SANOFANEL005) and pooled upon reception. Rat and

human liver microsomes and rat intestinal microsomes were purchased from Tebu-bio. Solvents were from common sources and of LC-MS grade.

Plasma/ Whole Blood stabilities

Plasma or whole blood incubations were performed in duplicate, at 37 °C, in Eppendorf tubes. The incubation contained 10 µM test compound (1% methanol) in rat or human plasma in a final volume of 0.5 mL. Sampling points were taken at 0, 15, 30, 60, 120, 240, 360 min and reactions were terminated by adding ice-cold methanol containing 500 nM internal standard (9 volumes). The samples were centrifuged for 10 min at 10000 g, 4 °C to pellet precipitated protein and the supernatant was transferred in Matrix tubes for LC-MS/MS analysis. Incubations with specific esterases inhibitors were performed in duplicate, at 37 °C, in Eppendorf tubes. The incubation contained 10 µM test compound (1% methanol) in rat or human plasma and the appropriate esterase inhibitor (1.25 mM PMSF, 0.25 mM BNPP, 1 mM DTNB, 0.05 mM profenamine, 0.5 mM EDTA or 0.5 mM huprine²), in a final volume of 0.5 mL. Sampling points were taken at 0, 15, 30, 60, 120, 240, 360 min and reactions were terminated by adding ice-cold methanol containing 500 nM internal standard (9 volumes). The samples were centrifuged for 10 min at 10000 g, 4 °C to pellet precipitated protein and the supernatant was transferred in Matrix tubes for LC-MS/MS analysis. Control incubations were performed in duplicate, with methanol instead of the inhibitor compound. Each experiment included a reference compound tested in the same conditions and allowing the validation of the experiment: eucatropine (10 µM, $t_{1/2}$ = 9 min, human plasma or whole blood) and enalapril (10 µM, $t_{1/2}$ = 13 min, rat plasma or whole blood).

Microsomal Stability

Microsomal incubations were performed in duplicate, at 37°C, in glass tubes. The incubation contained 1 µM test compound (1% methanol) in rat liver microsomes, human liver microsomes or rat intestinal microsomes (1mg of microsomal protein/mL) in a final volume of 0.25 mL. Sampling points were taken at 0, 15, 30, 60, 120 min and reactions were terminated by adding ice-cold methanol or acetonitrile containing 200 nM internal standard (4 volumes). The samples were centrifuged for 10 min at 10000g, 4°C to pellet precipitated microsomal protein and the supernatant was transferred in Matrix tubes for LC-MS/MS analysis. Control incubations were performed in triplicate, with denaturated microsomes with acetonitrile containing 200 nM internal standard and sampling points were taken at 0 min and 120 min (to evaluate the compound chemical stability in the experimental conditions). Each experiment included a reference compound tested in the same conditions and allowing the validation of the experiment:trandolapril ($t_{1/2}$ human = 20 min, $t_{1/2}$ rat = 7 min, 1µM, CES1 substrate) for liver microsomes and prasugrel ($t_{1/2}$ rat = 1 min, 1 µM, CES2 substrate) for intestinal microsomes.

LC-MS/MS analysis

Samples analysis were performed on a liquid chromatography coupled to a triple quadrupole mass spectrometer (Acquity I Class - Xevo TQD, Waters, Les Ulis, France) with an electrospray ionisation source. Chromatographic separations were carried out using an Acquity BEH C18, 1,7µm, 50 x 2.1mm column (Waters) maintained at 40°C. Mobile phase solvent A was 10 mM ammonium acetate in water and solvent B was acetonitrile with 0,1% of formic acid. The following gradient was applied: 2% B during 10s, 2-98% B in 1'50; hold at 98% B for 30s; 98%-2% B in 5s; 2% B hold for 1'30. The injection volume was 1 µL and the flow rate of 600 µL/min. The desolvation and cone gas flow were respectively 1200 and 50 L/h; the source temperature was 600°C. The capillary and cone voltages, the collision energy and the observed MRM transitions were automatically optimized for each compound.

Quantitation of each compound was achieved by conversion of the corresponding analyte/internal standard peak area ratios to percentage drug remaining, using the T0 ratio values as 100%. The slope of the linear regression from log percentage remaining versus incubation time relationships (-k) was used in the conversion to *in vitro* t_{1/2} values by: *in vitro* t_{1/2} = -0.693/k.

Statistical analysis

Half-lives were calculated using Xlfit™ (IDBS Ltd). Data for Box-Whisker plots were calculated using Microsoft Excel. Univariate and multivariate statistical analysis was performed using SPSS v19 (IBM, Armonk, NY).

AUTHOR INFORMATION

Corresponding Author

* R.D.P.: phone +33 (0)320 964 948; e-mail: rebecca.deprez@univ-lille2.fr

ORCID Rebecca Deprez-Poulain orcid.org/0000-0002-3318-5297

Author Contributions

These authors contributed equally.

ACKNOWLEDGMENT

We are grateful to the institutions that support our laboratory: INSERM, Université de Lille, Institut Pasteur de Lille. The authors thank Agathe Urban, Matthias Borms, Thomas Bosio for technical assistance. Foundation pour la Recherche Médicale (grant DCM20111223046) and Agence Nationale de la recherche (grant ANR-11-JS07-015-01) are thanked for funding. Paul Hermant is recipient of a doctoral fellowship of Conseil Régional Nord-Pas de Calais and INSERM. NMR acquisitions were done at the Laboratoire d'Application de Résonance Magnétique Nucléaire (LARMN), Lille, France. Rebecca Deprez-Poulain is a member of the Institut Universitaire de France.

ABBREVIATIONS

AChE, acetylcholinesterase; AGG, aggrecanase; aq., aqueous; ArE, arylesterase; BNPP, bis-(4-nitrophenyl)-phosphate; BoNTA, neurotoxin A metalloprotease of *bacterium Clostridium botulinum*; BuChE, butyrylcholinesterase; CES1, carboxylesterase-1; CES2, carboxylesterase-2; CNS, central nervous system; DIPEA, *N,N*-diisopropylethylamine; DMF, *N,N*-dimethylformamide; DTNB, 5,5'-dithiobis(2-nitrobenzoic acid) ; EDCI, *N*-(3-dimethylaminopropyl)-*N'*-ethylcarbodiimide hydrochloride; EDTA, ethylenediaminetetraacetic acid; equiv, equivalent; EtOH, ethanol; GCPII, glutamate carboxypeptidase II; HBTU, 2-(1H-benzotriazol-1-yl)-1,1,3,3-tetramethyluronium hexafluorophosphate; HCV, hepatitis C virus; HER-2, human epidermal growth factor receptor 2; HIV, human immunodeficiency virus; HOBt, hydroxybenzotriazole; IDE, insulin-degrading enzyme; LDA, lithium diisopropylamide; LpxC, UDP-3-*O*-(*R*-3-hydroxymyristoyl)-*N*-acetylglucosamine deacetylase; MeCN, acetonitrile; MeOH, methanol; MMP, matrix metalloprotease; OR, Odd-ratio ; PDF, peptide deformylase; PfAM1, *Plasmodium falciparum* aminopeptidase-1; PMSF, phenylmethanesulfonyl fluoride; PON-1, paraoxonase-1; profenamine, ethopropazine hydrochloride; ROCK, rho kinase; SA, serum albumin; TACE, tumor necrosis factor- α -converting enzyme; TFA, trifluoroacetic acid; THF, tetrahydrofuran; TIS, triisopropylsilane.

SUPPORTING INFORMATION

The Supporting Information is available free of charge on the ACS Publications website at DOI: XXX. Supplementary figures; Supplementary tables; Synthesis of intermediates; Molecular docking and scoring methods; (PDF).

References

1 Sieber, S. A.; Niessen, S.; Hoover, H. S.; Cravatt, B. F. Proteomic Profiling of Metalloprotease Activities with Cocktails of Active-Site Probes. *Nat. Chem. Biol.* **2006**, *2*, 274-281.

2 Marmion, C. J.; Griffith, D.; Nolan, K. B. Hydroxamic Acids - an Intriguing Family of Enzyme Inhibitors and Biomedical Ligands. *Eur. J. Inorg. Chem.* **2004**, *2004*, 3003-3016.

3 Boularot, A.; Giglione, C.; Petit, S.; Duroc, Y.; Alves de Sousa, R.; Larue, V.; Cresteil, T.; Dardel, F.; Artaud, I.; Meinnel, T. Discovery and Refinement of a New Structural Class of Potent Peptide Deformylase Inhibitors. *J. Med. Chem.* **2007**, *50*, 10-20.

4 Seki, H.; Pellett, S.; Šilhár, P.; Stowe, G. N.; Blanco, B.; Lardy, M. A.; Johnson, E. A.; Janda, K. D. Synthesis/Biological Evaluation of Hydroxamic Acids and Their Prodrugs as Inhibitors for Botulinum Neurotoxin a Light Chain. *Bioorg. Med. Chem.* **2014**, *22*, 1208–1217.

5 McAllister, L. A.; Montgomery, J. I.; Abramite, J. A.; Reilly, U.; Brown, M. F.; Chen, J. M.; Barham, R. A.; Che, Y.; Chung, S. W.; Menard, C. A.; Mitton-Fry, M.; Mullins, L. M.; Noe, M. C.; O'Donnell, J. P.; Oliver III, R. M.; Penzien, J. B.; Plummer, M.; Price, L. M.; Shanmugasundaram, V.; Tomaras, A. P.; Uccello, D. P. Heterocyclic Methylsulfone Hydroxamic Acid LpxC Inhibitors as Gram-Negative Antibacterial Agents. *Bioorg. Med. Chem. Lett.* **2013**, *22*, 6832-6838.

6 Ai, T.; Xu, Y.; Qiu, L.; Geraghty, R. J.; Chen, L. Hydroxamic Acids Block Replication of Hepatitis C Virus. *J. Med. Chem.* **2015**, *58*, 785-800.

7 Plewe, M. B.; Butler, S. L.; Dress, K.; Hu, Q.; Johnson, T. W.; Kuehler, J. E.; Kuki, A.; Lam, H.; Liu, W.; Nowlin, D.; Peng, Q.; Rahavendran, S. V.; Tanis, S. P.; Tran, K. T.; Wang, H.; Yang, A.; Zhang, J. Azaindole Hydroxamic Acids Are Potent Hiv-1 Integrase Inhibitors. *J. Med. Chem.* **2009**, *52*, 7211-7219.

8 (a) Deprez-Poulain, R.; Flipo, M.; Piveteau, C.; Leroux, F.; Dassonneville, S.; Florent, I.; Maes, L.; Cos, P.; Deprez, B. Structure-Activity Relationships and Blood Distribution of

Antiplasmodial Aminopeptidase-1 Inhibitors. *J. Med. Chem.* **2012**, *55*, 10909-10917. (b)

Mistry, S. N.; Drinkwater, N.; Ruggeri, C.; Sivaraman, K. K.; Loganathan, S.; Fletcher, S.; Drag, M.; Paiardini, A.; Avery, V. M.; Scammells, P. J.; McGowan, S. Two-Pronged Attack: Dual Inhibition of Plasmodium Falciparum M1 and M17 Metalloaminopeptidases by a Novel Series of Hydroxamic Acid-Based Inhibitors. *J. Med. Chem.* **2014**, *57*, 9168-9183.

9 France, D. J.; Stepek, G.; Houston, D. R.; Williams, L.; McCormack, G.; Walkinshaw, M. D.; Page, A. P. Identification and Activity of Inhibitors of the Essential Nematode-Specific Metalloprotease Dpy-31. *Bioorg. Med. Chem. Lett.* **2015**, *25*, 5752-5755.

10 Novakova, Z.; Wozniak, K.; Jancarik, A.; Rais, R.; Wu, Y.; Pavlicek, J.; Ferraris, D.; Havlinova, B.; Ptacek, J.; Vavra, J.; Hin, N.; Rojas, C.; Majer, P.; Slusher, B. S.; Tsukamoto, T.; Barinka, C. Unprecedented Binding Mode of Hydroxamate-Based Inhibitors of Glutamate Carboxypeptidase II: Structural Characterization and Biological Activity. *J. Med. Chem.* **2016**, *59*, 4539-4550.

11 Deprez-Poulain, R.; Hennuyer, N.; Bosc, D.; Liang, W. G.; Enée, E.; Marechal, X.; Charton, J.; Totobenazara, J.; Berte, G.; Jahklal, J.; Verdelet, T.; Dumont, J.; Dassonneville, S.; Woitrain, E.; Gauriot, M.; Paquet, C.; Duplan, I.; Hermant, P.; Cantrelle, F.-X.; Sevin, E.; Culot, M.; Landry, V.; Herledan, A.; Piveteau, C.; Lippens, G.; Leroux, F.; Tang, W.-J.; van Endert, P.; Staels, B.; Deprez, B. Catalytic Site Inhibition of Insulin-Degrading Enzyme by a Small Molecule Induces Glucose Intolerance in Mice. *Nat. Commun.* **2015**, *6*, 8250.

12 Orbe, J.; Sánchez-Arias, J. A.; Rabal, O.; Rodríguez, J. A.; Salicio, A.; Ugarte, A.; Belzunce, M.; Xu, M.; Wu, W.; Tan, H.; Ma, H.; Páramo, J. A.; Oyarzabal, J. Design, Synthesis, and Biological Evaluation of Novel Matrix Metalloproteinase Inhibitors as Potent Antihemorrhagic Agents: From Hit Identification to an Optimized Lead. *J. Med. Chem.* **2015**, *58*, 2465-2488.

13 Noe, M. C.; Natarajan, V.; Snow, S. L.; Mitchell, P. G.; Lopresti-Morrow, L.; Reeves, L. M.; Yocum, S. A.; Carty, T. J.; Barberia, J. A.; Sweeney, F. J.; Liras, J. L.; Vaughn, M.;

Hardink, J. R.; Hawkins, J. M.; Tokar, C. Discovery of 3,3-Dimethyl-5-Hydroxypipercolic Hydroxamate-Based Inhibitors of Aggrecanase and Mmp-13. *Bioorg. Med. Chem. Lett.* **2005**, *15*, 2808-2811.

14 Elbakali, J.; Gras, H.; Maingot, L.; Deprez, B.; Dumont, J.; Leroux, F.; Deprez-Poulain, R. Inhibition of Aggrecanase as a Therapeutic Strategy in Osteoarthritis. *Future Med. Chem.* **2014**, *6*, 1399-1412.

15 Zhu, Z.; Mazzola, R.; Sinning, L.; McKittrick, B.; Niu, X.; Lundell, D.; Sun, J.; Orth, P.; Guo, Z.; Madison, V.; Ingram, R.; Beyer, B. M. Discovery of Novel Hydroxamates as Highly Potent Tumor Necrosis Factor-Converting Enzyme Inhibitors: Part I: Discovery of Two Binding Modes. *J. Med. Chem.* **2008**, *51*, 725-736.

16 a) Ouvry, G.; Berton, Y.; Bhurruth-Alcor, Y.; Bonnary, L.; Bouix-Peter, C.; Bouquet, K.; Bourotte, M.; Chambon, S.; Comino, C.; Deprez, B.; Duvert, D.; Duvert, G.; Hacini-Rachinel, F.; Harris, C. S.; Luzy, A.-P.; Mathieu, A.; Millois, C.; Pascau, J.; Pinto, A.; Polge, G.; Reitz, A.; Reversé, K.; Rosignoli, C.; Taquet, N.; Hennequin, L. F. Identification of Novel Tace Inhibitors Compatible with Topical Application. *Bioorg. Med. Chem. Lett.* **2017**, *27*, 1848-1853. b) Boiteau, J.-G.; Ouvry, G.; Arlabosse, J.-M.; Astri, S.; Beillard, A.; Bhurruth-Alcor, Y.; Bonnary, L.; Bouix-Peter, C.; Bouquet, K.; Bourotte, M.; Cardinaud, I.; Comino, C.; Deprez, B.; Duvert, D.; Féret, A.; Hacini-Rachinel, F.; Harris, C. S.; Luzy, A.-P.; Mathieu, A.; Millois, C.; Orsini, N.; Pascau, J.; Pinto, A.; Piwnica, D.; Polge, G.; Reitz, A.; Reversé, K.; Rodeville, N.; Rossio, P.; Spiesse, D.; Tabet, S.; Taquet, N.; Tomas, L.; Vial, E.; Hennequin, L. F. Discovery and Process Development of a Novel Tace Inhibitor for the Topical Treatment of Psoriasis. *Bioorg. Med. Chem.*, [Online early access]. doi:10.1016/j.bmc.2017.07.054. Published Online: 2 August 2017. [URL](#) (accessed October 5th, 2017).

17 Yao, W.; Zhuo, J.; Burns, D. M.; Xu, M.; Zhang, C.; Li, Y. L.; Qian, D. Q.; He, C.; Weng, L.; Shi, E.; Lin, Q.; Agrios, C.; Burn, T. C.; Calder, E.; Covington, M. B.; Fridman, J. S.;

Friedman, S.; Katiyar, K.; Hollis, G.; Li, Y.; Liu, C.; Liu, X.; Marando, C. A.; Newton, R.; Pan, M.; Scherle, P.; Taylor, N.; Vaddi, K.; Wasserman, Z. R.; Wynn, R.; Yeleswaram, S.; Jalluri, R.; Bower, M.; Zhou, B. B.; Metcalf, B. Discovery of a Potent, Selective, and Orally Active Human Epidermal Growth Factor Receptor-2 Sheddase Inhibitor for the Treatment of Cancer. *J. Med. Chem.* **2007**, *50*, 603-606.

18 Falkenberg, K. J.; Johnstone, R. W. Histone Deacetylases and Their Inhibitors in Cancer, Neurological Diseases and Immune Disorders. *Nat. Rev. Drug Discovery* **2014**, *13*, 673-691.

19 Yang, S.-M.; Scannevin, R. H.; Wang, B.; Burke, S. L.; Huang, Z.; Karnachi, P.; Wilson, L. J.; Rhodes, K. J.; Lagu, B.; Murray, W. V. B-N-Biaryl Ether Sulfonamide Hydroxamates as Potent Gelatinase Inhibitors: Part 2. Optimization of A-Amino Substituents. *Bioorg. Med. Chem. Lett.* **2008**, *18*, 1140-1145.

20 Du, L.; Musson, D. G.; Wang, A. Q. Stability Studies of Vorinostat and Its Two Metabolites in Human Plasma, Serum and Urine. *J. Pharm. Biomed. Anal.* **2006**, *42*, 556-564.

21 Kitamura, S.; Sugihara, K.; Tatsumi, K. Reductase Activity of Aldehyde Oxidase toward the Carcinogen N-Hydroxy-2-Acetylaminofluorene and the Related Hydroxamic Acids. *Biochem. Mol. Biol. Int.* **1994**, *34*, 1197-1203.

22 (a) Mulder, G. J.; Meerman, J. H. Sulfation and Glucuronidation as Competing Pathways in the Metabolism of Hydroxamic Acids: The Role of N,O-Sulfonation in Chemical Carcinogenesis of Aromatic Amines. *Environ. Health Perspect.* **1983**, *49*, 27-32.; (b) Song, D.; Lee, C.; Kook, Y. J.; Oh, S. J.; Kang, J. S.; Kim, H.-J.; Han, G. Improving Potency and Metabolic Stability by Introducing an Alkenyl Linker to Pyridine-Based Histone Deacetylase Inhibitors for Orally Available Runx3 Modulators. *Eur. J. Med. Chem.* **2017**, *126*, 997-1010..

23 Lassalas, P.; Gay, B.; Lasfargeas, C.; James, M. J.; Tran, V.; Vijayendran, K. G.; Brunden, K. R.; Kozlowski, M. C.; Thomas, C. J.; Smith, A. B., 3rd; Hury, D. M.; Ballatore, C. Structure Property Relationships of Carboxylic Acid Isosteres. *J. Med. Chem.* **2016**, *59*, 3183-3203.

24 Flipo, M.; Charton, J.; Hocine, A.; Dassonneville, S.; Deprez, B.; Deprez-Poulain, R. Hydroxamates: Relationships between Structure and Plasma Stability. *J. Med. Chem.* **2009**, *52*, 6790-6802.

25 Calvo, E.; Reddy, G.; Boni, V.; Garcia-Canamaque, L.; Song, T.; Tjornelund, J.; Choi, M. R.; Allen, L. F. Pharmacokinetics, Metabolism, and Excretion of (14)C-Labeled Belinostat in Patients with Recurrent or Progressive Malignancies. *Invest. New Drugs* **2016**, *34*, 193-201.

26 Hajduk, P. J.; Shuker, S. B.; Nettlesheim, D. G.; Craig, R.; Augeri, D. J.; Betebenner, D.; Albert, D. H.; Guo, Y.; Meadows, R. P.; Xu, L.; Michaelides, M.; Davidsen, S. K.; Fesik, S. W. Nmr-Based Modification of Matrix Metalloproteinase Inhibitors with Improved Bioavailability. *J. Med. Chem.* **2002**, *45*, 5628-5639.

27 Fukami, T.; Yokoi, T. The Emerging Role of Human Esterases. *Drug Metab. Pharmacokinet.* **2012**, *27*, 466-477.

28 Casey Laizure, S.; Herring, V.; Hu, Z.; Witbrodt, K.; Parker, R. B. The Role of Human Carboxylesterases in Drug Metabolism: Have We Overlooked Their Importance? *Pharmacotherapy* **2013**, *33*, 210-222.

29 Hwang, S.-K.; Juhasz, A.; Yoon, S.-H.; Bodor, N. Soft Drugs. 12. Design, Synthesis, and Evaluation of Soft Bufuralol Analogues. *J. Med. Chem.* **2000**, *43*, 1525-1532.

30 Boland, S.; Bourin, A.; Alen, J.; Geraets, J.; Schroeders, P.; Castermans, K.; Kindt, N.; Boumans, N.; Panitti, L.; Fransen, S.; Vanormelingen, J.; Stassen, J. M.; Leysen, D.; Defert, O. Design, Synthesis, and Biological Evaluation of Novel, Highly Active Soft Rock Inhibitors. *J. Med. Chem.* **2015**, *58*, 4309-4324.

31 Lockridge, O.; Xue, W.; Gaydess, A.; Grigoryan, H.; Ding, S. J.; Schopfer, L. M.; Hinrichs, S. H.; Masson, P. Pseudo-Esterase Activity of Human Albumin: Slow Turnover on Tyrosine 411 and Stable Acetylation of 82 Residues Including 59 Lysines. *J. Biol. Chem.* **2008**, *283*, 22582-22590.

- 32 Harel, M.; Aharoni, A.; Gaidukov, L.; Brumshtein, B.; Khersonsky, O.; Meged, R.; Dvir, H.; Ravelli, R. B.; McCarthy, A.; Toker, L.; Silman, I.; Sussman, J. L.; Tawfik, D. S. Structure and Evolution of the Serum Paraoxonase Family of Detoxifying and Anti-Atherosclerotic Enzymes. *Nat. Struct. Mol. Biol.* **2004**, *11*, 412-419.
- 33 Montella, I. R.; Schama, R.; Valle, D. The Classification of Esterases: An Important Gene Family Involved in Insecticide Resistance--a Review. *Mem. Inst. Oswaldo Cruz* **2012**, *107*, 437-449.
- 34 Yamaori, S.; Fujiyama, N.; Kushihara, M.; Funahashi, T.; Kimura, T.; Yamamoto, I.; Sone, T.; Isobe, M.; Ohshima, T.; Matsumura, K.; Oda, M.; Watanabe, K. Involvement of Human Blood Arylesterases and Liver Microsomal Carboxylesterases in Nafamostat Hydrolysis. *Drug Metab. Pharmacokinet.* **2006**, *21*, 147-155.
- 35 Ronco, C.; Foucault, R.; Gillon, E.; Bohn, P.; Nachon, F.; Jean, L.; Renard, P.-Y. New Huprine Derivatives Functionalized at Position 9 as Highly Potent Acetylcholinesterase Inhibitors. *ChemMedChem* **2011**, *6*, 876-888.
- 36 Imai, T.; Taketani, M.; Shii, M.; Hosokawa, M.; Chiba, K. Substrate Specificity of Carboxylesterase Isozymes and Their Contribution to Hydrolase Activity in Human Liver and Small Intestine. *Drug Metab. Dispos.* **2006**, *34*, 1734-1741.
- 37 Minagawa, T.; Kohno, Y.; Suwa, T.; Tsuji, A. Species Differences in Hydrolysis of Isocarbacyclin Methyl Ester (Tei-9090) by Blood Esterases. *Biochem. Pharmacol.* **1995**, *49*, 1361-1365.
- 38 Rudakova, E. V.; Boltneva, N. P.; Makhaeva, G. F. Comparative Analysis of Esterase Activities of Human, Mouse, and Rat Blood. *Bull. Exp. Biol. Med.* **2011**, *152*, 73-75.
- 39 Bahar, F. G.; Ohura, K.; Ogihara, T.; Imai, T. Species Difference of Esterase Expression and Hydrolase Activity in Plasma. *J. Pharm. Sci.* **2012**, *101*, 3979-3988.

40 Hosokawa, M. Structure and Catalytic Properties of Carboxylesterase Isozymes Involved in Metabolic Activation of Prodrugs. *Molecules* **2008**, *13*, 412-431.

41 Li, B.; Sedlacek, M.; Manoharan, I.; Boopathy, R.; Duysen, E. G.; Masson, P.; Lockridge, O. Butyrylcholinesterase, Paraoxonase, and Albumin Esterase, but Not Carboxylesterase, Are Present in Human Plasma. *Biochem. Pharmacol.* **2005**, *70*, 1673-1684.

42 Meshorer, E.; Soreq, H. Virtues and Woes of Ache Alternative Splicing in Stress-Related Neuropathologies. *Trends Neurosci.* **2006**, *29*, 216-224.

43 Polasek, T. M.; Doogue, M. P.; Miners, J. O. Metabolic Activation of Clopidogrel: In Vitro Data Provide Conflicting Evidence for the Contributions of Cyp2c19 and Pon1. *Ther. Adv. Drug Saf.* **2011**, *2*, 253-261.

44 Eng, H.; Niosi, M.; McDonald, T. S.; Wolford, A.; Chen, Y.; Simila, S. T.; Bauman, J. N.; Warmus, J.; Kalgutkar, A. S. Utility of the Carboxylesterase Inhibitor Bis-Para-Nitrophenylphosphate (Bnpp) in the Plasma Unbound Fraction Determination for a Hydrolytically Unstable Amide Derivative and Agonist of the Tgr5 Receptor. *Xenobiotica* **2010**, *40*, 369-380.

45 Warmus, J. S.; Quinn, C. L.; Taylor, C.; Murphy, S. T.; Johnson, T. A.; Limberakis, C.; Ortwine, D.; Bronstein, J.; Pagano, P.; Knafels, J. D.; Lightle, S.; Mochalkin, I.; Brideau, R. and Podoll, T. Structure-Based Design of an *in vivo* Active Hydroxamic Acid Inhibitor of *P. aeruginosa* LpxC. *Bioorg. Med. Chem. Lett.* **2012**, *22*, 2536-2543.

46 (a) Cheng, X.-C.; Wang, R.-L.; Dong, Z.-K.; Li, J.; Li, Y.-Y. and Li, R.-R. Design, Synthesis and Evaluation of Novel Metalloproteinase Inhibitors Based on L-Tyrosine Scaffold. *Bioorg. Med. Chem.* **2012**, *20*, 5738-5744; (b) Tamura, Y.; Watanabe, F.; Nakatani, T.; Yasui, K.; Fuji, M.; Komurasaki, T.; Tsuzuki, H.; Maekawa, R.; Yoshioka, T.; Kawada, K.; Sugita, K. and Ohtani, M. Highly Selective and Orally Active Inhibitors of Type IV Collagenase (MMP-9 and MMP-2): N-Sulfonylamino Acid Derivatives. *J. Med. Chem.* **1998**, *41*, 640-649; (c) Supuran,

C. T. and Scozzafava, A. Protease inhibitors. Part 7: Inhibition of *Clostridium histolyticum* Collagenase with Sulfonylated Derivatives of L-Valine Hydroxamate. *Eur. J. Pharm. Sci.* **2000**, *10*, 67-76. (d) MacPherson, L. J.; Bayburt, E. K.; Capparelli, M. P.; Carroll, B. J.; Goldstein, R.; Justice, M. R.; Zhu, L.; Hu, S.; Melton, R. A.; Fryer, L.; Goldberg, R. L.; Doughty, J. R.; Spirito, S.; Blancuzzi, V.; Wilson, D.; O'Byrne, E. M.; Ganu, V. and Parker, D. T. Discovery of CGS 27023A, a Non-Peptidic, Potent, and Orally Active Stromelysin Inhibitor That Blocks Cartilage Degradation in Rabbits. *J. Med. Chem.* **1997**, *40*, 2525-2532; (e) Dankwardt, S. M.; Abbot, S. C.; Broka, C. A.; Martin, R. L.; Chan, C. S.; Springman, E. B.; Van Wart, H. E. and Walker, K. A. M. Amino Acid Derived Sulfonamide Hydroxamates as Inhibitors of Procollagen C-Proteinase. Part 2: Solid-Phase Optimization of Side Chains. *Bioorg. Med. Chem. Lett.* **2002**, *12*, 1233-1235.

47 Elbakali, J.; Gras, H.; Maingot, L.; Deprez, B.; Dumont, J.; Leroux, F.; Deprez-Poulain, R. Inhibition of Aggrecanase as a Therapeutic Strategy in Osteoarthritis. *Future Med. Chem.* **2014**, *6*, 1399-1412.

48 Clary, L.; Pascal, j.-C. 4-Alkoxy-N- (2-Hydroxycarbamoyl-2-Piperidinyl-Ethyl) - Benzamide Compounds as Selective Tace-Inhibitors for the Treatment of Inflammatory Diseases. WO2011033010 (A1) March 24, 2011.

49 Finn, P. W.; Bandara, M.; Butcher, C.; Finn, A.; Hollinshead, R.; Khan, N.; Law, N.; Murthy, S.; Romero, R.; Watkins, C.; Andrianov, V.; Bokaldere, R. M.; Dikovska, K.; Gailite, V.; Loza, E.; Piskunova, I.; Starchenkov, I.; Vorona, M. and Kalvinsh, I. Novel Sulfonamide Derivatives as Inhibitors of Histone Deacetylase. *Helv. Chim. Acta* **2005**, *88*, 1630-1657.

50 Wang, H.; Yu, N.; Chen, D.; Lee, K. C. L.; Lye, P. L.; Chang, J. W. W.; Deng, W.; Ng, M. C. Y.; Lu, T.; Khoo, M. L.; Poulsen, A.; Sangthongpitag, K.; Wu, X.; Hu, C.; Goh, K. C.; Wang, X.; Fang, L.; Goh, K. L.; Khng, H. H.; Goh, S. K.; Yeo, P.; Liu, X.; Bonday, Z.; Wood, J. M.; Dymock, B. W.; Kantharaj, E.; Sun, E. T. Discovery of (2e)-3-{2-Butyl-1-[2-

(Diethylamino)Ethyl]-1h-Benzimidazol-5-Yl}-N-Hydroxyacrylamide (Sb939), an Orally Active Histone Deacetylase Inhibitor with a Superior Preclinical Profile. *J. Med. Chem.* **2011**, *54*, 4694-4720.

51 Reiter, L. A.; Robinson, R. P.; McClure, K. F.; Jones, C. S.; Reese, M. R.; Mitchell, P. G.; Otterness, I. G.; Bliven, M. L.; Liras, J.; Cortina, S. R.; Donahue, K. M.; Eskra, J. D.; Griffiths, R. J.; Lame, M. E.; Lopez-Anaya, A.; Martinelli, G. J.; McGahee, S. M.; Yocum, S. A.; Lopresti-Morrow, L. L.; Tobiassen, L. M.; Vaughn-Bowser, M. L. Pyran-Containing Sulfonamide Hydroxamic Acids: Potent Mmp Inhibitors That Spare Mmp-1. *Bioorg. Med. Chem. Lett.* **2004**, *14*, 3389-3395.

52 Matter, H.; Schudok, M.; Schwab, W.; Thorwart, W.; Barbier, D.; Billen, G.; Haase, B.; Neises, B.; Weithmann, K.-U.; Wollmann, T. Tetrahydroisoquinoline-3-Carboxylate Based Matrix-Metalloproteinase Inhibitors: Design, Synthesis and Structure–Activity Relationship. *Bioorg. Med. Chem.* **2002**, *10*, 3529-3544.

53 Murphy-Benenato, K. E.; Olivier, N.; Choy, A.; Ross, P. L.; Miller, M. D.; Thresher, J.; Gao, N.; Hale, M. R. Synthesis, Structure, and Sar of Tetrahydropyran-Based Lpxc Inhibitors. *ACS Med. Chem. Lett.* **2014**, *5*, 1213-1218.

54 Ott, G. R.; Asakawa, N.; Lu, Z.; Liu, R.-Q.; Covington, M. B.; Vaddi, K.; Qian, M.; Newton, R. C.; Christ, D. D.; Traskos, J. M.; Decicco, C. P.; Duan, J. J. W. A,B-Cyclic-B-Benzamido Hydroxamic Acids: Novel Templates for the Design, Synthesis, and Evaluation of Selective Inhibitors of Tnf-A Converting Enzyme (Tace). *Bioorg. Med. Chem. Lett.* **2008**, *18*, 694-699.

55 Yang, S.-M.; Lagu, B.; Wilson, L. J. Mild and Efficient Lewis Acid-Promoted Detritylation in the Synthesis of N-Hydroxy Amides: A Concise Synthesis of (–)-Cobactin T. *J. Org. Chem.* **2007**, *72*, 8123-8126.

56 Levy, D. E.; Lapierre, F.; Liang, W.; Ye, W.; Lange, C. W.; Li, X.; Grobelny, D.; Casabonne, M.; Tyrrell, D.; Holme, K.; Nadzan, A.; Galaray, R. E. Matrix Metalloproteinase Inhibitors: A Structure–Activity Study. *J. Med. Chem.* **1998**, *41*, 199-223.

57 Ho, C. Y.; Strobel, E.; Ralbovsky, J.; Galembo, R. A. Improved Solution- and Solid-Phase Preparation of Hydroxamic Acids from Esters. *J. Org. Chem.* **2005**, *70*, 4873-4875.

58 Harris, T. L.; Worthington, R. J.; Melander, C. A Facile Synthesis of 1,5-Disubstituted-2-Aminoimidazoles: Antibiotic Activity of a First Generation Library. *Bioorg. Med. Chem. Lett.* **2011**, *21*, 4516-4519.

59 Boldt, G. E.; Kennedy, J. P.; Janda, K. D. Identification of a Potent Botulinum Neurotoxin a Protease Inhibitor Using in Situ Lead Identification Chemistry. *Org. Lett.* **2006**, *8*, 1729-1732.

60 Xu, D.; Lu, C.; Chen, W. Palladium-Catalyzed Double Arylations of Terminal Olefins in Acetic Acid. *Tetrahedron* **2012**, *68*, 1466-1474.

61 Ramachary, D. B.; Venkaiah, C.; Reddy, Y. V.; Kishor, M. Multi-Catalysis Cascade Reactions Based on the Methoxycarbonylketene Platform: Diversity-Oriented Synthesis of Functionalized Non-Symmetrical Malonates for Agrochemicals and Pharmaceuticals. *Org. Biomol. Chem.* **2009**, *7*, 2053-2062.

62 Berry, L. M.; Wollenberg, L.; Zhao, Z. Esterase Activities in the Blood, Liver and Intestine of Several Preclinical Species and Humans. *Drug Metab. Lett.* **2009**, *3*, 70-77.

Table of Contents Graphic

